Engravings on bone from the archaic hominin site of Lingjing (Xuchang, Henan, China)

Zhanyang Li, Luc Doyon, Hao Li, Qiang Wang, Zhongqiang Zhang, Qingpo Zhao, Francesco D'errico

Engravings on bone from the archaic hominin site of Lingjing (Xuchang, Henan, China)

LI, ZhanYang[1,2], DOYON, Luc[1,3], LI, Hao[4,5], WANG, Qiang[1], ZHANG, ZhongQiang[1], ZHAO, QingPo[1,2], d'ERRICO, Francesco[3,6*]

[1]Institute of Cultural Heritage, Shandong University, 27 Shanda Nanlu, Hongjialou District, Jinan 250100, China.
[2]Henan Provincial Institute of Cultural Relics and Archaeology, 9 3rd Street North, LongHai Road, Guancheng District, Zhenzhou 450000, China.
[3]Centre National de la Recherche Scientifique, UMR 5199 – PACEA, Université de Bordeaux, Bât. B18, Allée Geoffroy Saint Hilaire, CS 50023, 33615 Pessac CEDEX, France.
[4]Key Laboratory of Vertebrate Evolution and Human Origins, Institute of Vertebrate Paleontology and Paleoanthropology, Chinese Academy of Sciences, 142 Xizhimenwai Street, Xicheng District, Beijing 100044, China.
[5]CAS Center for Excellence in Life and Paleoenvironment, 142 Xizhimenwai Street, Xicheng District, Beijing 100044, China
[6]SFF Centre for Early Sapiens Behaviour (SapienCE), University of Bergen, Øysteinsgate 3, Postboks 7805, 5020, Bergen, Norway.

*Author for correspondence (Email: francesco.derrico@u-bordeaux.fr)

Keywords: East Asia; Late Pleistocene; Symbolism; Art; Ochre

Abstract

The production of abstract engravings is considered an indicator of modern cognition and a mean for recording and transmitting information in a durable manner. We report the discovery of two engravings found at the Lingjing site (Henan, China), dated to 105-125kya, which has also yielded important hominin remains. The patterns consist of carefully engraved incisions on weathered rib fragments, excluding the possibility of an unintentional or utilitarian origin. Chemical analysis of residues inside the lines of one

specimen identifies ochre. Our results suggest ochred engravings were deliberately used for symbolic purposes by East Asian early Late Pleistocene hominins.

Introduction

Opinions differ between those who think archaic hominins' cognition was comparable to that of contemporaneous modern humans (d'Errico & Stringer 2011; Hovers & Belfer-Cohen 2006; Nowell 2010; Villa & Roebroeks 2014; Zilhão 2011), and those who think morphological (Bruner 2014; Pearce *et al.* 2013), physiological (de Boer 2012; Lieberman 2007; Spoor *et al.* 2003), ontogenetic (Gunz *et al.* 2010; Neubauer 2015), and behavioural (Benazzi *et al.* 2011; Junker 2010; Mellars 2010) differences suggest a different cognitive setting. The first viewpoint is supported by the fact that the emergence of our species in Africa, *c.* 300kya (Hublin *et al.* 2017; Stringer 2016; Grün *et al.* 1996), was not immediately accompanied by the development of behaviours characteristic of historically documented populations. For tens of thousands of years after their emergence, anatomically modern human populations in Africa continued to use technologies that differed little from those of the non-modern populations preceding them or inhabiting other regions inside and outside the African continent at the time. It is also supported by the discovery of cultural innovations generally considered as hallmarks of modern cognition among archaic populations of Eurasia. Burials, collection of fossils and other rare objects, production of engraved patterns, pigment use, cave painting, personal ornaments, extraction of bird feathers and claws are interpreted as the proof that Neanderthals in Europe and the Near East engaged in symbolically mediated behaviour (e.g. Finlayson *et al.* 2012; Hoffmann *et al.* 2018; Peresani *et al.* 2011; Pettitt 2002; Radovčić *et al.* 2015; Rodríguez-Vidal *et al.* 2014; Romandini *et al.* 2014; Zilhão *et al.* 2010). Most of these innovative cultural adaptations are however virtually unknown in vast regions inhabited by archaic hominins before the arrival of modern human populations, in particular East Asia.

Abstract engravings are reported from almost forty African and Eurasian sites dated prior to 40kya (OSM 1, and references therein). The earliest examples are the engraved patterns on a freshwater shell from Trinil at 540kya, a bone from Bilzingsleben at 370kya (but see Müller & Pasda 2011), ochre fragments from Klasies River, Pinnacle Point, and Blombos Cave at 110–73kya and an antler from Vaufrey at 120kya. In China, engraved

objects from Pleistocene contexts are rare. The earliest possible example is a *Stegodon* ivory tusk found in a layer dated between 120–150kya at Xinglongdong cave, South China. It displays few longitudinal incisions close to the tusk tip. However, the chronology of the site and the anthropogenic nature of the incisions were questioned (Norton & Jin 2009) as elephants use their tusks in a variety of activities, which could result in their breakage, and the development of ground facets and incisions (Haynes 1991; Villa & d'Errico 2001). A pebble bearing a set of sub-parallel and intersecting lines comes from Shuidonggou Locality 1, Lower Cultural Unit, dated to *c.* 40kya. An engraved antler comes from Zhoukoudian Upper Cave (Pei 1934), now dated to between 34–29kya (Chen *et al.* 1992). Initially described as engraved, a bone flake recovered at Shiyu site, Shanxi Province, from a layer dated between 32–28kya (You 1984) is probably bearing post-depositional surface modifications (Bednarik 1994). Finally, an antler fragment with an engraved pattern consisting of sinuous parallel lines is reported from Longgu cave, Hebei Province, dated to 13kya (Bednarik & You 1991). Here we report on the discovery of deliberately engraved lines on weathered bone fragments, in one case filled with ochre, found at the 105–125kya site of Lingjing in China. They were found in the same geological layer that yielded hominin remains attributed to an archaic population exhibiting a mosaic of anatomical features suggestive of complex population dynamics between Eastern and Western Eurasia (Li *et al.* 2017). It was recently suggested that Lingjing hominins were Denisovans (Martinón-Torres *et al*. 2017: S444) although palaeogenetic evidence is lacking at this time to corroborate this hypothesis.

Archaeological Context

Lingjing (34° 04′ 08.6″ N, 113° 40′ 47.5″ E, elev. 117 m) is an open-air site located in the Henan Province, northern China, about 120km south of the Yellow River (Figure 1). The site, a water-lain deposit, was discovered in 1965. Since 2005, 551m^2 were excavated under the supervision of one of us (LZ). The 9m deep sedimentary sequence comprises eleven geological layers (OSM 2 for details). Three main archaeological horizons attest the human occupation of the site during the Holocene (layers 1-4), the LGM to the Younger Dryas (layer 5), and the early Late Pleistocene (layers 10-11). OSL ages from layer 11 indicate a deposition taking place at *c.* 125–105 kya (Nian *et al.* 2009), i.e. during the early

phases of MIS5 (MIS5e to MIS5d). *Equus caballus*, *Equus hemionus*, and *Bos primigenius* dominate the faunal assemblage from layer 11. Skeletal elements from late Middle and early Late Pleistocene fauna were also identified (Li & Dong 2007). The high proportion of limb bones (>60%) and the high frequency of cut-marks on midshafts (~34%) suggest Lingjing layer 11 was a kill-butchery site (Zhang *et al.* 2012).

The lithic assemblage is mostly composed of quartz and quartzite artefacts. The presence of cores, flakes, formal tools, debris, the identification of use wear on some artefacts (Li 2007), and of bone retouchers (Doyon *et al.* 2018) suggest knapping activities including tool manufacture and use occurred at the site. The two engraved bone fragments described in this study come from layer 11. They were discovered in 2009 (n° 9L0141 and 9L0148) and identified by some of us (LZ, LH, LD, FD) as engraved during an analysis of the faunal assemblage conducted in 2016.

Methods

Excavation methods at Lingjing involve removing the sediments with curved-tipped trowels to avoid damaging the finds, 3-D plotting of bone remains and lithic artefacts, and sediment sieving with a 2-mm mesh. Lithic and faunal remains are cleaned under running water with soft brushes. When present, concretions are not removed from the faunal remains.

The artefacts described in this study are curated at the Henan Provincial Institute for Cultural Relics and Archaeology, ZhengZhou, China. Permission from this institution was granted to analyse one object (9L0141) at the Raman and Scanning Electron Microscopy Facilities of the Shandong University's Institute of Measurement and Testing. The four aspects of the specimens were examined, and photographed with a Canon PowerShot 100 and a Nikon D300 AF Micro Nikkor 60 mm f/2.8D. Microscopic analysis was conducted with a Leica Wild M3C stereomicroscope equipped with a Nikon CoolPix 900 Digital Camera at magnifications ranging from 4x to 40x. Data on the morphology (section, start and end line morphology), and occurrence of technological features (internal striations, breaks, side striations, changes in direction) were recorded as well as the presence of red residue. Identification of the origin of modifications on bone is based on criteria inferred from the experimental reproduction and microscopic analysis of sequential marks

produced on bone objects with different tools and motions (d'Errico 1995; Fritz 1999).

A sample of 227 bone fragments from the 2005-2015 excavations with no or few concretions was examined under microscope. The following variables were recorded on the specimens bearing undisputable cut marks (Noe-Nygaard 1987; Fisher 1995; Lyman 1994; Fernández-Jalvo & Andrews 2016): number, arrangement (divergent, overlapping, parallel, sub-parallel), morphology (curved, sinuous, straight), edge morphology (clean, fringed), occurrence of side striations, conspicuous changes in direction, surface micro-breaks, and presence of red-residue.

A selected area on the engraved aspect of specimen 9L0141 was replicated with Coltene President regular body dental elastomer (Coltène, Switzerland). The negative replica was analysed with a Sensofar S-Neox confocal microscope driven by the SensoScan 6 software (Sensofar, Barcelona). Data was processed with the SensoMap 7.3 software. Specimen 9L0141 and sediment sample trapped in the spongy bone were analysed with SEM-EDS and Raman spectroscopy. Sediment from layer 11 were analysed with ED-XRF (OSM 3 for details).

Results

Taphonomic analysis. Bone surfaces not affected by taphonomic processes or coated by concretions are exceptionally well preserved. Cut marks are the main anthropogenic modification recorded on the faunal assemblage (23.79%; Figure 2, OSM 4). They are present on all skeletal elements, including ribs (12.96%). They show morphological traits typical of cut marks on fresh bone and exceptional changes in direction (OSM 4). Root etching affects about one fifth of the analysed sample (22.03%). Carnivore gnawing and etching resulting from digestion by carnivore affect respectively 3.96% and 2.20% of the sample. Other modifications include percussion marks, possibly for marrow extraction (3.52%), traces of utilization as retouchers (3.08%), and staining produced by heat (1.32%). No red residue was detected on the faunal remains included in the comparative sample.

Microscopic analysis. Specimen 9L0141 is too fragmentary to propose a firm taxonomic attribution based on morphology (Figure 3A). The thickness and flatness of the cortical

bone, and the morphology of the spongy tissue suggest it belongs to the distal portion of an adult large-sized mammal rib. The periosteal surface displays a pronounced fibrous structure consisting of alternating sub-parallel grooves and ridges (OSM 7). The four fractures are ancient, as indicated by a slight smoothing of their edges and prominent areas visible under the microscope. Their morphology and orientation indicate they occurred on weathered bone (Lyman 1994; Villa & Mahieu 1991). Seven sub-parallel lines cross the periosteal surface (Figure 4A). The abrupt terminations of L1 and L2 and the lower terminations of L3-L5 indicate they were interrupted by the adjacent fractures (Figure 5A, OSM 6). The upper terminations of L3-L5 were engraved when the piece was already fragmented (OSM 6). L6 and L7 are complete. The grainy appearance of the lines' surface (Figure 6), their micro-fringed outlines, and step micro-fractures produced when incising natural ridges (OSM 6) suggest they were engraved on weathered bone (OSM 5).

The lines' depth remains constant when crossing the micro-grooves and ridges composing the fibrous periosteal surface (L1-L5) (Figure 5A-B). The section of the bone surface shows the grooves vary between 50-100µm in depth and 100-600µm in width (OSM 6), indicating the tool tip was extremely sharp, and not wider than 50-100µm. Momentary loss of control of the engraver's motion due to tool speed changes when crossing the natural bone surface undulations (d'Errico 1994; d'Errico 1995) is indicated by frequent sudden changes of direction on L1-L6 (Figure 5B-C). L1-L5 were engraved by a single passage of the tool. L6-L7 are composed of respectively three and five close, parallel, and discontinuous striations produced each by a single passage of the point (OSM 6).

Similarities in section and width indicate that L1-L2 were engraved by the same point, creating a narrow groove with a flat bottom (Figure 5A). L3-L5 were also produced by a same point generating a wider and shallower groove with similar internal striations, and side-striations on both sides of the main line. The multiple striations composing L6-L7 were probably made by the same tool used for L3-L5, which however marked the bone more superficially (OSM 6). The difference in morphology between L1-L2 and L3-L7 can either be attributed to a tool change or to the wear or breakage of the point used to engrave L1-L2.

The location of the micro-fractures on the ridges indicates the lines were engraved from the longer to the shorter edge of the bone (Figure 5A, OSM 7). The sections of well-

defined lines are asymmetrical to the right (OSM 5), which is indicative, considering the motion direction, of a right-handed engraver (Bosinski *et al.* 2002; d'Errico *et al.* 2018). Right-handed engravers generally create sequences of parallel lines by juxtaposing them from left to right (d'Errico 1992). This would favour the interpretation that the morphological change between L1-L2 and L3-L7 resulted from the wear or breakage of the tool.

Specimen 9L0148 is a rib fragment from an adult large-sized mammal (Figure 3B). The flat periosteal surface displays chemical etching whitening at places the bone surface (Figure 7A), removal of primary bone lamellae, and parallel sets of thin striations owing to trampling. The top, bottom, and left fractures are eroded and fringed; those on the right side are fresher, indicating the fragment underwent at least two breakage events. Ten sub-parallel lines (L1-L10) perpendicular to the object main axis cross the periosteal surface (Figure 4B). They were produced before the breakage of the rib (OSM 5). Their narrowness, similar internal morphology, and the absence of side striations demonstrate they were engraved by the same sharp lithic point in a single session (Figure 7B). Slight changes in direction when crossing micro-fractures and areas damaged by taphonomic processes, and their irregular outline suggest the lines were engraved on weathered bone. They were traced with a quick motion toward the wider edge of the object as indicated by the thin terminations of L6-L10.

Residue analysis. Abundant microscopic red residues were detected on specimen 9L0141 inside lines L2, L4-L6, and adjacent to lines L3-L6 (Figure 4A, OSM 7). Such residues are undetected under optical microscope in the whitish sediment trapped in the spongy bone opposite to the engraved surface (OSM 7).

The Raman analysis of red residues inside the lines produces a composite spectrum with seven peaks at 225, 293, 411, 497, 612, 1242, and 1271 cm^{-1} (OSM 7). The five peak values in the low frequencies identify haematite (de Faria *et al.* 1997).

Raman analysis of particles composing the sediment trapped in the spongy bone only identifies quartz and a single instance of a particle containing haematite (OSM 7). SEM-EDS analysis reveals the sediment comprises particles ranging from 20-200 µm in size and is mainly composed of mica, either muscovite or biotite, embedded in a clay matrix

containing small proportions of iron (Fe), magnesium (Mg), and calcium (Ca). Single instances of quartz grain, zircon, bone fragment, and iron-rich particle are also detected (OSM 7). ED-XRF analysis of sediment from layer 11 confirms that silicon (Si) represents the main chemical element followed by aluminum (Al), and potassium (K), with iron (Fe) accounting only for 2.4-2.6% (OSM 7).

Discussion and conclusion

The lines on specimens 9L0141 and 9L0148 cannot result from excavation, cleaning or curation of the faunal remains discovered at Lingjing. They are different in a number of respects from cut-marked bones found in layer 11 at this site. Cut marks on the latter generally show microscopic features demonstrating they were made on fresh bone. Sets of close cut marks made in rapid succession by the same cutting edge rarely exceed four. Usually, they slightly diverge from a focal point and keep a similar outline. Lines on the two specimens, and more evidently for those on 9L0141, were traced on partially weathered fragments, and several lines on this last specimen were engraved when the bone was already fragmented. On 9L0141, the lines were produced by an extremely sharp point, and the prehistoric author applied him/herself when engraving the first five lines to carefully mark the bone surface despite its highly rugged topography. To make the following lines visible, he/she marked them with multiple strokes. As a whole, this evidence is inconsistent with an interpretation of the lines on 9L0141 as resulting from butchery activities. It rather suggests a deliberate engraving of the bone. Although less striking, the lines on 9L0148 differ from cut-marks on faunal remains from the same layer in their number, morphology, and the tool used to produce them. Furthermore, chemical alteration of the periosteal surface damaging some lines indicates they are ancient in origin, and cannot be attributed to neither excavation nor curation.

The numerous haematite-rich residues inside four lines on 9L0141 and the virtual absence of iron-rich particles in the clay sediment composing layer 11 is puzzling. Considering the chemical composition of layer 11 and the extreme rarity and small size of iron-rich particles, one would have expected to find white residues composed of clay and micas at the bottom of the engraved lines. The absence of white sediment and presence instead of haematite-rich deposits in the lines and recessed areas close to them may have

resulted from smearing ochre powder on the bone surface to highlight the engraved pattern and increase its visibility. This practice is common in Upper Palaeolithic mobiliary art (Buisson *et al.* 1989; García *et al.* 2016). The use of ochre to modify the appearance of personal ornaments is already attested at 80 ka BP Middle Stone Age sites (d'Errico *et al.* 2009). In China, the earliest evidence for the use of ochre comes from Zhoukoudian Upper Cave, and Shuidonggou Locality 2 and 8 in form of modified lumps and ornaments coloured with ochre (Pitarch Martí *et al.* 2017).

A growing body of evidence from Europe and Southeast Asia (Supplementary, Table 1) supports the hypothesis that archaic hominins cultural adaptations involved symbolically mediated behaviour, therefore challenging the idea that modern cognitive abilities are restricted to *Homo sapiens*. While many authors now agree with this point of view for Neanderthals, no evidence was supporting, before this study, that the same may apply to Denisovans, the possible makers of the engravings described in our study. The Lingjing engravings represent the first possible example of such behaviour in Eastern Asia which predates 40kya, and was studied by taking into account contextual data, the taphonomy of the associated faunal assemblage, and conducting an in-depth analysis of the objects. The deliberate nature of the markings on 9L0141, and likely on 9L0148, as well as the application of ochre on the former do not identify in itself the purpose of these practices. It is, however, fully consistent with the hypothesis that a meaning could have been attributed to the patterns or to the action producing them. We are still far from understanding the purpose of these engravings for the archaic human groups living in China during the early Late Pleistocene. Only future finds may identify spatiotemporal consistencies giving clues for fully evaluating their significance. Future excavations will also be instrumental to establish whether these objects were more often disposed or lost, or have a better chance to survive, at semi-residential sites close to active water springs. The recent identification of bone and antler fragments used to retouch lithics from the same layer that has yielded the engraved specimens analyzed here shows the Lingjing visitors knew the mechanical properties of weathered bone and considered it as a raw material suitable to produce artefacts (Doyon *et al.* 2018). The Lingjing engravings suggest they also saw bone as a media on which they could permanently record sequential markings, and ochre as a substance that helped in highlighting them.

Acknowledgement

We thank Alain Queffelec (CNRS – UMR5199 PACEA) and François-Xavier Le Bourdonnec (CNRS – UMR5060 IRAMAT-CRP2A) for their help with the sediment analyses. The scientific research at Lingjing is funded by grants from the National Natural Science Foundation of China (41630102, 41672020) and Shandong University 111 Project (111-2-09). The present study was funded by the Sino-French Cai Yuanpei program (36707NF). LH acknowledges the support from the Chinese Academy of Sciences Pioneer Hundred Talents Program. This work was partially supported by the Research Council of Norway through its Centre's of Excellence funding scheme, SFF Centre for Early Sapiens Behaviour (SapienCE), project number 262618. LD was granted financial support from the Institut écologie et environnement of the Centre national de la recherche scientifique (CNRS-InEE). PACEA (UMR5199 CNRS) is a Partner team of the Labex LaScArBx-ANR n° ANR-10-LABX-52

References

BEDNARIK, R.G. 1994. The Pleistocene art of Asia. *Journal of World Prehistory* 8: 351–375.

BEDNARIK, R.G., Y. YOU 1991. Palaeolithic art from China. *Rock Art Research* 8: 119–123.

BENAZZI, S., K. DOUKA, C. FORNAI, C.C. BAUER, O. KULLMER, J. SVOBODA, I. PAP, F. MALLEGNI, P. BAYLE, M. COQUERELLE, S. CONDEMI, A. RONCHITELLI, K. HARVATI & G.W. WEBER. 2011. Early dispersal of modern humans in Europe and implications for Neanderthal behaviour. *Nature* 479: 525–528.

BOSINSKI, G., F. D'ERRICO & P. SCHILLER. 2002. *Die gravierten Frauendarstellungen von Gönnersdorf*. Stuttgart: Franz Steiner Verlag.

BRUNER, E. 2014. Functional craniology, human evolution, and anatomical constraints in the Neanderthal braincase, in T. Akazawa, N. Ogihara, H.C. Tanabe, & H. Terashima (ed.) *Dynamics of learning in Neanderthals and modern humans Volume 2*: 121–129. Tokyo: Springer.

BUISSON, D., M. MENU, G. PINÇON & P. WALTER. 1989. Les objets colorés du Paléolithique supérieur: cas de la grotte de La Vache (Ariège). *Bulletin de la Société préhistorique française* 86: 183–191.

CHEN, T., R.E.M. HEDGES & Z. YUAN. 1992. New AMS 14C dating on Upper Cave and relative issues. *Acta Anthropologica Sinica* 11: 112–115.

D'ERRICO, F. 1992. Technology, motion, and the meaning of Epipaleolithic art. *Current Anthropology* 33: 94–109.

— 1994. *L'art gravé azilien : de la technique à la signification*. Paris: CNRS Éditions.

— 1995. Image analysis and 3-D optical surface profiling of Upper Palaeolithic mobiliary art. *Microscopy and analysis* 51: 27–29.

D'ERRICO, F., L. DOYON, I. COLAGÉ, A. QUEFFELEC, E. LE VRAUX, G. GIACOBINI, B. VANDERMEERSCH & B. MAUREILLE. 2018. From number sense to number symbols: an archaeological perspective. *Philosophical Transactions of the Royal Society B* 373: 20160518.

D'ERRICO, F. & C.B. STRINGER. 2011. Evolution, revolution or saltation scenario for the emergence of modern cultures? *Philosophical Transactions of the Royal Society B* 366: 1060–1069.

D'ERRICO, F., M. VANHAEREN, N. BARTON, A. BOUZOUGGAR, H. MIENIS, D. RICHTER, J.-J. HUBLIN, S.P. MCPHERRON & P. LOZOUET. 2009. Additional evidence on the use of personal ornaments in the Middle Paleolithic of North Africa. *Proceedings of the National Academy of Sciences* 106: 16051–16056.

DE BOER, B. 2012. Loss of air sacs improved hominin speech abilities. *Journal of Human Evolution* 62: 1–6.

DE FARIA, D.L.A., S. VENÂNCIO SILVA & M.T. DE OLIVEIRA. 1997. Raman microspectroscopy of some iron oxides and oxyhydroxides. *Journal of Raman Spectroscopy* 28: 873–878.

DOYON, L., Z. LI, L. HAO & F. D'ERRICO. 2018. Discovery of *circa* 115,000-year-old bone retouchers at Lingjing, Henan, China. *PLOS ONE* 13: e0194318.

FERNÁNDEZ-JALVO, Y. & P. ANDREWS. 2016. *Atlas of taphonomic identifications*. New York: Springer.

FINLAYSON, C., K. BROWN, R. BLASCO, J. ROSELL, J.J. NEGRO, G.R. BORTOLOTTI, G. FINLAYSON, A. SÁNCHEZ MARCO, F. GILES PACHECO, J. RODRÍGUEZ VIDAL, J.S. CARRIÓN, D.A. FA & J.M. RODRÍGUEZ LLANES. 2012. Birds of a feather: Neanderthal exploitation of raptors and corvids. *PLOS ONE* 7: e45927.

FISHER, J.W. 1995. Bone surface modifications in zooarchaeology. *Journal of Archaeological Method and Theory* 2: 7–68.

FRITZ, C. 1999. Towards the reconstruction of Magdalenian artistic techniques: the contribution of microscopic analysis of mobiliary art. *Cambridge Archaeological Journal* 9: 189–208.

GARCÍA, C.R., V.V. BONILLA, I.R. MARÍN & S.M. MASCARÓS. 2016. A unique collection of Palaeolithic painted portable art: characterization of red and yellow pigments from the Parpalló Cave (Spain). *PLOS ONE* 11: e0163565.

GRÜN, R., J.S. BRINK, N.A. SPOONER, L. TAYLOR, C.B. STRINGER, R.G. FRANCISCUS & A.S. MURRAY. 1996. Direct dating of Florisbad hominid. *Nature* 382: 500–501.

GUNZ, P., S. NEUBAUER, B. MAUREILLE & J.-J. HUBLIN. 2010. Brain development after birth differs between Neanderthals and modern humans. *Current Biology* 20: R921–R922.

HAYNES, G. 1991. *Mammoths, mastodonts, and elephants: biology, behavior and the fossil record*. Cambridge: Cambridge University Press.

HOFFMANN, D.L., C.D. STANDISH, M. GARCÍA-DIEZ, P.B. PETTITT, J.A. MILTON, J. ZILHÃO, J.J. ALCOLEA-GONZÁLEZ, P. CANTALEJO-DUARTE, H. COLLADO, R. de BALBÍN, M. LORBLANCHET, J. RAMOS-MUÑOZ, G.-C. WENIGER & A.W.G. PIKE. 2018. U-Th dating of carbonate crusts reveals Neandertal origin of Iberian cave art. *Science* 359: 912–915.

HOVERS, E. & A. BELFER-COHEN. 2006. "Now you see it, now you don't": modern human behavior in the Middle Paleolithic, in E. Hovers & S.L. Kuhn (ed.) *Transitions before the transition*: 295–304. Boston: Springer.

HUBLIN, J.-J., A. BEN-NCER, S.E. BAILEY, S.E. FREIDLINE, S. NEUBAUER, M.M. SKINNER, I. BERGMANN, A. LE CABEC, S. BENAZZI, K. HARVATI & P. GUNZ. 2017. New fossils from Jebel Irhoud, Morocco and the pan-African origin of *Homo sapiens*. *Nature* 546: 289–292.

JUNKER, T. 2010. Art as a biological adaptation, or: why modern humans replaced the Neanderthals. *Quartär* 57: 171–178.

LI, Z. 2007. A primary study on the stone artifacts of Lingjing site excavated in 2005. *Acta Anthropologica Sinica* 26: 138–154.

LI, Z. & W. DONG. 2007. Mammalian fauna from the Lingjing Paleolithic site in Xuchang, Henan province. *Acta Anthropologica Sinica* 26: 345–360.

LI, Z., X. WU, L. ZHOU, W. LIU, X. GAO, X. NIAN & E. TRINKAUS. 2017. Late Pleistocene archaic human crania from Xuchang, China. *Science* 355: 969–972.

LIEBERMAN, P. 2007. The evolution of human speech: its anatomical and neural bases. *Current Anthropology* 48: 39–66.

LYMAN, R.L. 1994. *Vertebrate taphonomy*. New York: Cambridge University Press.

MARTINÓN-TORRES, M, X. WU, J.M. BERMÚDEZ DE CASTRO, S. XING & W. LIU. 2017. *Homo sapiens* in the Eastern Asian Late Pleistocene. *Current Anthropology* 58: S434–S448.

MELLARS, P. 2010. Neanderthal symbolism and ornament manufacture: the bursting of a bubble? *Proceedings of the National Academy of Sciences* 107: 20147–20148.

MÜLLER, W. & C. PASDA. 2011. Site formation and faunal remains of the Middle Pleistocene site Bilzingsleben. *Quartär* 58: 25–49.

NEUBAUER, S. 2015. Human brain evolution: ontogeny and phylogeny, in E. Bruner (ed.) *Human paleoneurology*: 95–120. Cham: Springer.

NIAN, X.M., L.P. ZHOU & J.T. QIN. 2009. Comparisons of equivalent dose values obtained with different protocols using a lacustrine sediment sample from Xuchang, China. *Radiation Measurements* 44: 512–516.

NOE-NYGAARD, N. 1987. Taphonomy in archaeology with special emphasis on man as a biasing factor. *Journal of Danish Archaeology* 6: 7–62.

NORTON, C.J. & J.J.H. JIN. 2009. The evolution of modern human behavior in East Asia: current perspectives. *Evolutionary Anthropology* 18: 247–260.

NOWELL, A. 2010. Defining behavioral modernity in the context of Neandertal and anatomically modern human populations. *Annual Review of Anthropology* 39: 437–452.

PEARCE, E., C. STRINGER & R.I.M. DUNBAR. 2013. New insights into differences in brain organization between Neanderthals and anatomically modern humans. *Proceedings of the Royal Society of London B* 280: 20130168.

PEI, W.C. 1934. A preliminary report on the Late Palaeolithic cave of Choukoutien. *Acta Geologica Sinica* 13: 327–358.

PERESANI, M., I. FIORE, M. GALA, M. ROMANDINI & A. TAGLIACOZZO. 2011. Late Neandertals and the intentional removal of feathers as evidenced from bird bone taphonomy at Fumane Cave 44 ky B.P., Italy. *Proceedings of the National Academy of Sciences* 108: 3888–3893.

PETTITT, P. 2002. The Neanderthal dead: exploring mortuary variability in Middle Palaeolithic Eurasia. *Before Farming* 2002: 1–26.

PITARCH MARTÍ, A., Y. WEI, X. GAO, F. CHEN & F. D'ERRICO. 2017. The earliest evidence of coloured ornaments in China: the ochred ostrich eggshell beads from Shuidonggou Locality 2. *Journal of Anthropological Archaeology* 48: 102–113.

RADOVČIĆ, D., A.O. SRŠEN, J. RADOVČIĆ & D.W. FRAYER. 2015. Evidence for Neandertal jewelry: modified white-tailed eagle claws at Krapina. *PLOS ONE* 10: e0119802.

RODRÍGUEZ-VIDAL, J., F. D'ERRICO, F.G. PACHECO, R. BLASCO, J. ROSELL, R.P. JENNINGS, A. QUEFFELEC, G. FINLAYSON, D.A. FA, J.M.G. LÓPEZ, J.S. CARRIÓN, J.J. NEGRO, S. FINLAYSON, L.M. CÁCERES, M.A. BERNAL, S.F. JIMÉNEZ & C. FINLAYSON. 2014. A rock engraving made by Neanderthals in Gibraltar. *Proceedings of the National Academy of Sciences* 111: 13301–13306.

ROMANDINI, M., M. PERESANI, V. LAROULANDIE, L. METZ, A. PASTOORS, M. VAQUERO & L. SLIMAK. 2014. Convergent evidence of eagle talons used by late Neanderthals in Europe: a further assessment on symbolism. *PLOS ONE* 9: e101278.

SPOOR, F., J.-J. HUBLIN, M. BRAUN & F. ZONNEVELD. 2003. The bony labyrinth of Neanderthals. *Journal of Human Evolution* 44: 141–165.

STRINGER, C. 2016. The origin and evolution of *Homo sapiens*. *Philosophical Transactions of the Royal Society B* 371: 20150237.

VILLA, P. & F. D'ERRICO. 2001. Bone and ivory points in the Lower and Middle Paleolithic of Europe. *Journal of Human Evolution* 41: 69–112.

VILLA, P. & E. MAHIEU. 1991. Breakage patterns of human long bones. *Journal of Human Evolution* 21: 27–48.

VILLA, P. & W. ROEBROEKS. 2014. Neandertal demise: an archaeological analysis of the modern human superiority complex. *PLOS ONE* 9: e96424.

YOU, Y.Z. 1984. Preliminary study of a Palaeolithic bone engraving. *Kexue Tongbao* 29: 80–82.

ZHANG, S., Z. LI, Y. ZHANG & X. GAO. 2012. Skeletal element distributions of the large herbivores from the Lingjing site, Henan province, China. *Science China: Earth Sciences* 55: 246–253.

ZILHÃO, J. 2011. Aliens from outer time? Why the "human revolution" is wrong, and where do we go from here?, in S. Condemi & G.-C. Weniger (ed.) *Continuity and Discontinuity in the Peopling of Europe*: 331–366. Dordrecht: Springer.

ZILHÃO, J., D.E. ANGELUCCI, E. BADAL-GARCÍA, F. D'ERRICO, F. DANIEL, L. DAYET, K. DOUKA, T.F.G. HIGHAM, M.J. MARTÍNEZ-SÁNCHEZ, R. MONTES-BERNÁRDEZ, S. MURCIA-MASCARÓS, C. PÉREZ-SIRVENT, C. ROLDÁN-GARCÍA, M. VANHAEREN, V. VILLAVERDE, R. WOOD & J. ZAPATA. 2010. Symbolic use of marine shells and mineral pigments by Iberian Neandertals. *Proceedings of the National Academy of Sciences* 107: 1023–1028.

Captions

Figure 1 (A) Location of Lingjing (Henan, China); (B) Stratigraphy indicating the geological and cultural layers (after Doyon *et al.* 2018).

Figure 2 Well-preserved sets of cut marks on faunal remains from Lingjing, layer 11. Scale = 1cm.

Figure 3 Photographs of engraved specimens (A) 9L0141, and (B) 9L0148.

448 **Figure 4** Photographs and tracing of the engraving on specimens (A) 9L0141, and (B)
449 9L0148. Red dots in (A) indicate the location of red residues.
450 **Figure 5** Microscopic photographs of engraved lines on specimen 9L0141. Changes in
451 direction of lines crossing the fibrous structure of the bone indicate the use of point
452 (A-B). Red residues are present inside the engraved lines (C).
453 **Figure 6** SEM photograph of specimen 9L0141 showing the grainy, slightly eroded
454 appearance of L4. Scale = 100µm.
455 **Figure 7** Close-up view of (A) L6, (B) L7 and L8 on specimen 9L0148. (A) Chemical etching
456 affecting the bone surface subsequent to the engraving. (B) Similar internal
457 morphology indicating the use of the same tool. Scales: (A) = 1mm; (B) = 500µm.
458

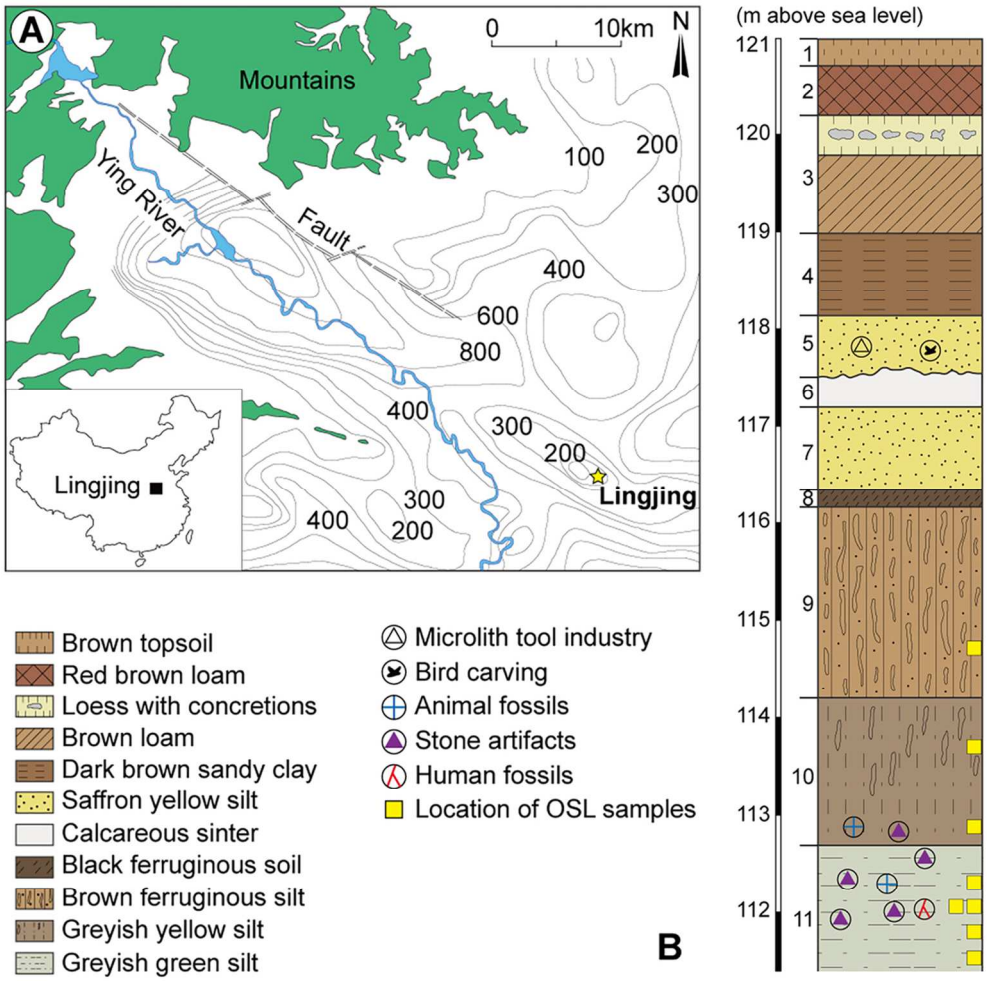

Figure 1 (A) Location of Lingjing (Henan, China); (B) Stratigraphy indicating the geological and cultural layers (after Doyon et al. 2018).

109x109mm (300 x 300 DPI)

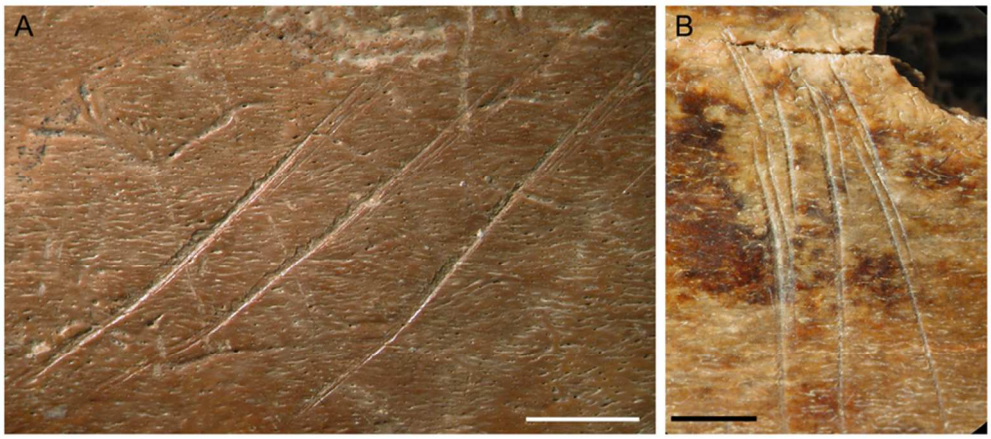

Figure 2 Well-preserved sets of cut marks on faunal remains from Lingjing, layer 11. Scale = 1cm.

75x33mm (300 x 300 DPI)

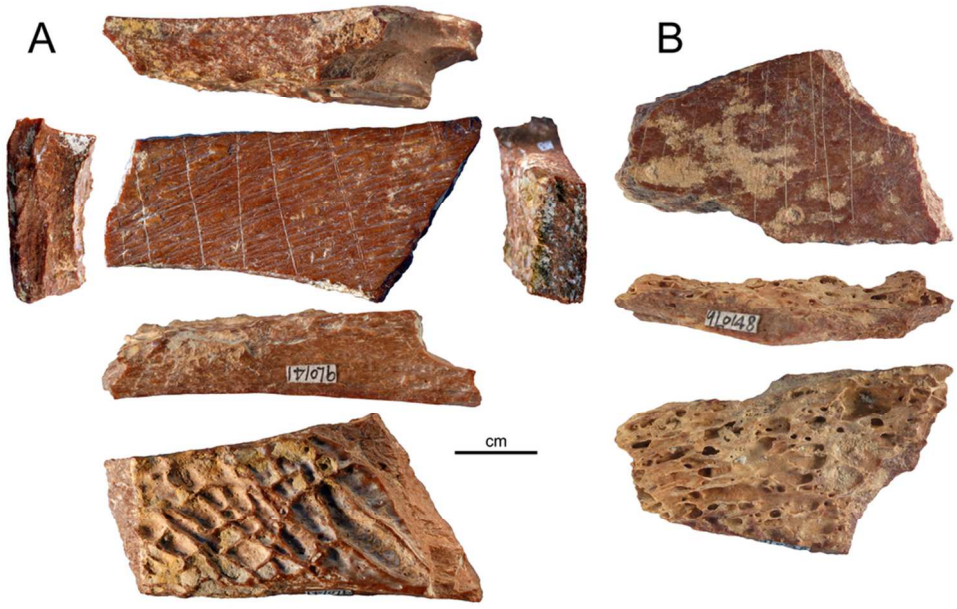

Figure 3 Photographs of engraved specimens (A) 9L0141, and (B) 9L0148.

88x55mm (300 x 300 DPI)

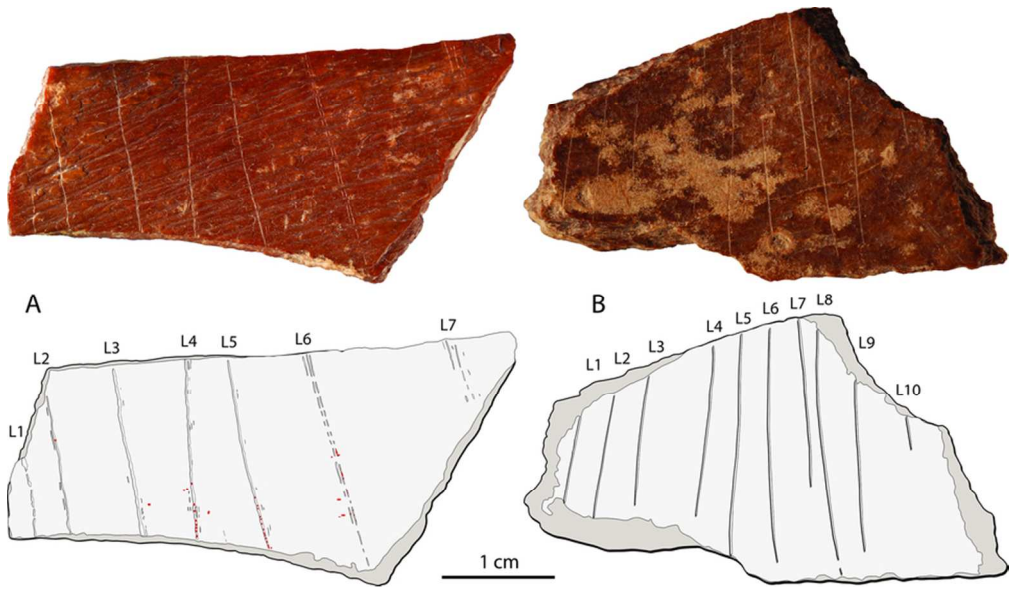

Figure 4 Photographs and tracing of the engraving on specimens (A) 9L0141, and (B) 9L0148. Red dots in (A) indicate the location of red residues.

81x47mm (300 x 300 DPI)

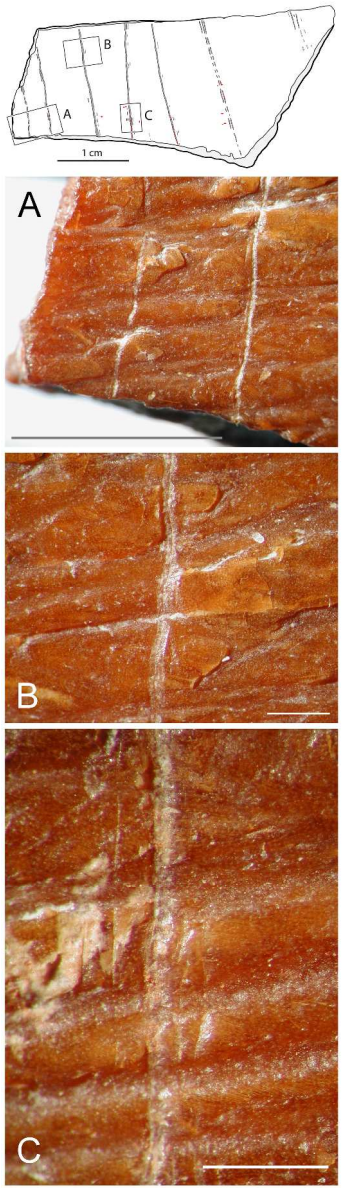

Figure 5 Microscopic photographs of engraved lines on specimen 9L0141. Changes in direction of lines crossing the fibrous structure of the bone indicate the use of point (A-B). Red residues are present inside the engraved lines (C).

164x577mm (300 x 300 DPI)

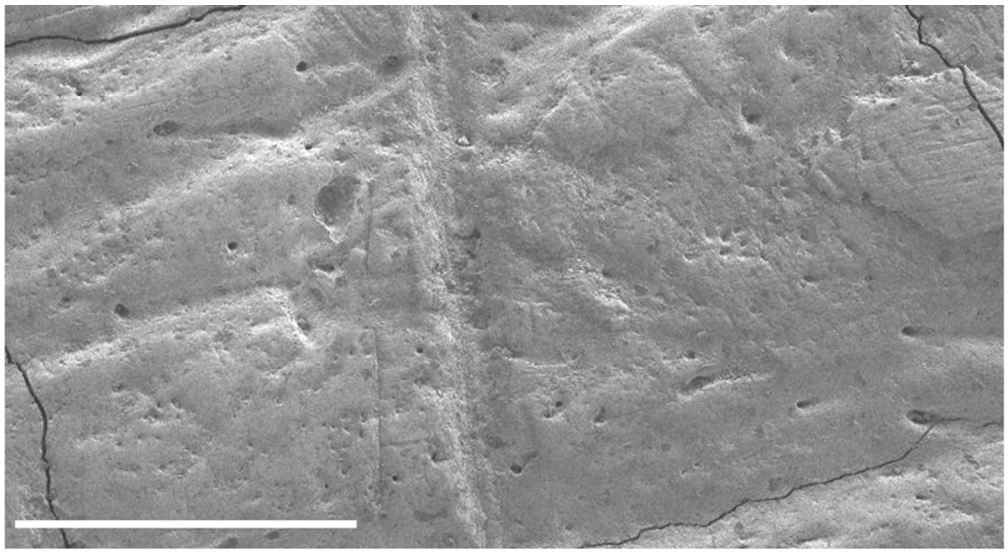

Figure 6 SEM photograph of specimen 9L0141 showing the grainy, slightly eroded appearance of L4. Scale = 100µm.

99x54mm (200 x 200 DPI)

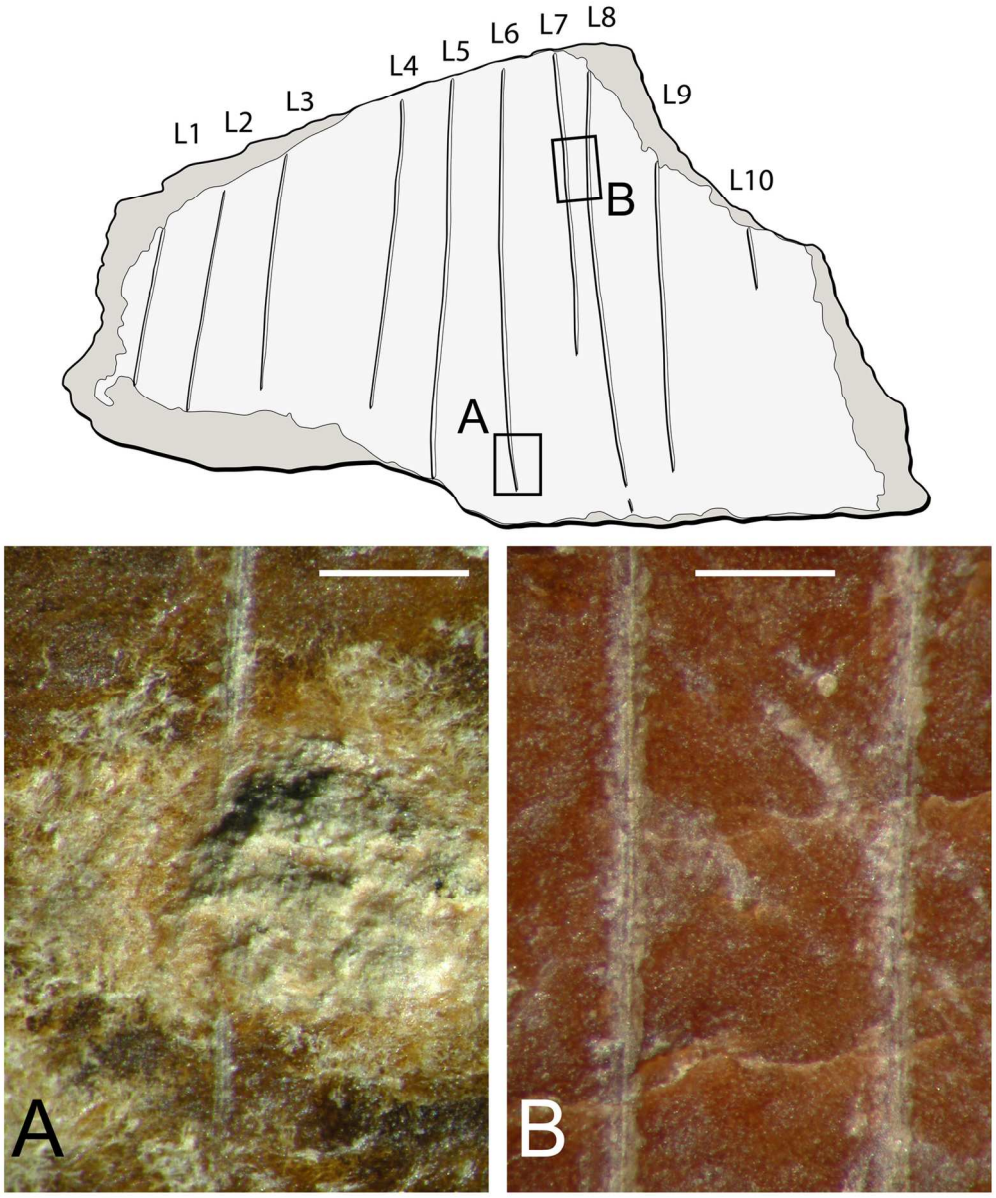

Figure 7 Close-up view of (A) L6, (B) L7 and L8 on specimen 9L0148. (A) Chemical etching affecting the bone surface subsequent to the engraving. (B) Similar internal morphology indicating the use of the same tool. Scales: (A) = 1mm; (B) = 500µm.

139x168mm (300 x 300 DPI)

Engravings on bone from the archaic hominin site of Lingjing (Xuchang, Henan, China)

LI, ZhanYang[1,2], DOYON, Luc[1,3], LI, Hao[4,5], WANG Qiang[1], ZHANG, ZhongQiang[1], ZHAO, QingPo[1,2], d'ERRICO, Francesco[3,6]

[1]Institute of Cultural Heritage, Shangong University, 27 Shanda Nanlu, Hongjialou District, Jinan 250100, China.
[2]Henan Provincial Institute of Cultural Relics and Archaeology, 9 3rd Street North, LongHai Road, Guancheng District, Zhenzhou 450000, China.
[3]Centre National de la Recherche Scientifique, UMR 5199 – PACEA, Université de Bordeaux, Bât. B18, Allée Geoffroy Saint Hilaire, CS 50023, 33615 Pessac CEDEX, France.
[4]Key Laboratory of Vertebrate Evolution and Human Origins, Institute of Vertebrate Paleontology and Paleoanthropology, Chinese Academy of Sciences, 142 Xizhimenwai Street, Xicheng District, Beijing 100044, China.
[5]CAS Center for Excellence in Life and Paleoenvironment, 142 Xizhimenwai Street, Xicheng District, Beijing 100044, China
[6]SFF Centre for Early Sapiens Behaviour (SapienCE), University of Bergen, Øysteinsgate 3, Postboks 7805, 5020, Bergen, Norway.

Online Supplementary Material

Table of contents

Online Supplementary Material 1: Early engravings from Africa and Eurasia

Table 1 Early engravings from Europe, Asia, and Africa (modified from Majkić *et al.* 2018a, 2018b).

Archaeological site	Country	Continent	Material	Cultural attribution	Age (kya)	Reference
Apollo 11	Namibia	Africa	Bone	MSA	71	(Vogelsang *et al.* 2010)
Blombos	South Africa	Africa	Ochre; Bone	MSA	100-75	(Henshilwood *et al.* 2002; 2009)
Border Cave	South Africa	Africa	Bone	ELSA	44-42	(d'Errico, Backwell, *et al.* 2012; d'Errico *et al.* 2018)
Diepkloof	South Africa	Africa	OES	MSA	65-55	(Texier *et al.* 2010)
Klasies River	South Africa	Africa	Ochre	MSA	100-85	(d'Errico, García Moreno, *et al.* 2012)
Klein Kliphuis	South Africa	Africa	Ochre	MSA	80-50	(Mackay & Welz 2008)
Klipdrift Shelter	South Africa	Africa	OES	MSA	65–59	(Henshilwood *et al.* 2014)
Pinnacle Point	South Africa	Africa	Ochre	MSA	100	(Watts 2010)
Sibudu Cave	South Africa	Africa	Ochre; Bone	MSA	77-58; 56-29	(Cain 2004; Hodgskiss 2014)
Shuidonggou Loc. 1	China	Asia	Pebble	C&F	40	(Peng *et al.* 2012)
Xinglongdong	China	Asia	Tusk	C&F	120-150	(Gao *et al.* 2004)
Trinil	Indonesia	Asia	Shell	LP	540-430	(Joordens *et al.* 2015)
Mar-Tarik	Iran	Asia	Slab	MP-M	123	(Jaubert *et al.* 2009)
Qafzeh	Israel	Asia	Flint	MP-M	100	(Hovers *et al.* 1997)
Quneitra	Israel	Asia	Flint	MP-M	60	(d'Errico, Henshilwood, *et al.* 2003; Goren-Inbar 1990)
Bacho Kiro	Bulgaria	Europe	Bone	MP-M	>47	(Bahn & Vertut 1997; Marshack 1976)
Kozarnika	Bulgaria	Europe	Bone	LP	900	(Sirakov *et al.* 2010)
Temnata Dupka	Bulgaria	Europe	Stone slab	MP	50	(Crémades *et al.* 1995)
Krapina	Croatia	Europe	Bone	MP	130	(Frayer *et al.* 2006)
Champlost Cave	France	Europe	Flint	MP-M	MIS3	(L'Homme & Normand 1993)
Chez Pourré-Chez Comte	France	Europe	Pebble	MP-M	MIS3	(L'Homme & Normand 1993)
Grotte du Renne	France	Europe	Bone	C	41-36	(d'Errico *et al.* 1998; d'Errico, Julien, *et al.* 2003; Zilhão 2007)
La Chapelle Aux Saints	France	Europe	Bone	MP-LM	60	(d'Errico *et al.* 2009; Langley *et al.* 2008)
La Ferrassie	France	Europe	Bone	MP-M	65	(Capitan & Peyrony 1912; Zilhão 2007)
Le Moustier	France	Europe	Bone	MP-M	40	(Langley *et al.* 2008)
Marillac	France	Europe	Bone	MP-LM	46	(d'Errico *et al.* 1998; 2009; 2018; Maureille *et al.* 2010)
Roc de Combe	France	Europe	Bone	C	40	(d'Errico *et al.* 1998)

Archaeological site	Country	Continent	Material	Cultural attribution	Age (kya)	Reference
Roche au Loup	France	Europe	Bone	C	40	(d'Errico *et al.* 1998)
Terra Amata	France	Europe	Pebble	LP	380	(Bourdier 1967; Leonardi 1976)
Vaufrey	France	Europe	Bone	MP-M	120 ± 10	(d'Errico *et al.* 2009; Vincent 1988)
Bilzingsleben	Germany	Europe	Bone	LP	412-320	(Mania & Mania 1988)
Gorham`s Cave	Gibraltar	Europe	Bedrock	MP-M	>39	(Rodríguez-Vidal *et al.* 2014)
Tata	Hungary	Europe	Shell	MP-M	>70	(Marshack 1976; 1990)
Grotta di Fumane	Italy	Europe	Flint; Pebble	MP-M	MIS5,4 & 3	(Leonardi 1981; Peresani *et al.* 2014)
Grotta Maggiore di San Bernardino	Italy	Europe	Flint	MP-M	59-44	(Peresani *et al.* 2014)
Riparo Tagliente	Italy	Europe	Flint; Pebble	MP-M	MIS3	(Leonardi 1983; 1988; Peresani *et al.* 2014)
Pešturina	Serbia	Europe	Bone	MP-Ch/Qt	95–64	(Majkić *et al.* 2018a)
Axlor	Spain	Europe	Pebble	MP	47.5	(García-Diez *et al.* 2013)
Grotta del Cavallo	Spain	Europe	Flint; Slab; Pebble	MP-M	MIS3	(Buggiani *et al.* 2004)
Grotta dell'Alto	Spain	Europe	Pebble	MP-M	MIS3	(Borzatti von Löwenstern & Magaldi 1967)
Kiik-Koba	Ukraine	Europe	Flint	MP-PM	32	(Stepanchuk 2006; Majkić *et al.* 2018b)
Prolom II	Ukraine	Europe	Bone	MP	41-28	(Stepanchuk 1993)
Zaskalnaya V	Ukraine	Europe	Ochre	MP-M	>47	(Stepanchuk 2006)

Material: OES = Ostrich Egg Shell
Cultural attribution: C = Chatelperronian; C&F = Cores and flates technology; Ch/Qt = Charentian Quina Type; ELSA = early Late Stone Age; LM = Late Mousterian; LP = Lower Paleolithic; M = Mousterian; MP = Middle Paleolithic; MSA = Middle Stone Age; PM = para-Micoquian

Online Supplementary Material 2: Site description

Lingjing (34° 04′ 08.6″ N, 113° 40′ 47.5″ E, elev. 117 m) is an open-air site located in northeast Xuchang county, Henan Province, northern China, about 120 km south of the Yellow River (Fig. 1). The site, a water-lain deposit, was discovered in 1965 when microblades, microcores (Chen 1983), and faunal remains were found on the surface (Z. Li, Wu, *et al.* 2017). Since 2005, 551m^2 was excavated under the supervision of one of us (LZ). The site features a 9m deep sedimentary sequence comprising eleven geological layers. The sequence includes from the top to the bottom: layers 1-4, Holocene in age, with material culture spanning from the Shang-Zhou Bronze Age to the Neolithic; layer 5 (yellowish silt), LGM to the Younger Dryas, with microblade technology, microcores, bone artefacts, perforated ostrich eggshells, ochre, faunal remains and the first evidence of pottery appearing in the region (Z. Li & Ma 2016; Z. Li, Kunikita, *et al.* 2017); layer 6 (flowstone layer), sterile; layer 7 (yellowish silt), sterile; layer 8 (black ferruginous soil), sterile; layer 9 (brownish ferruginous silt), sterile; layer 10 (brownish ferruginous silt), early Late Pleistocene with lithic artefacts and faunal remains (H. Li *et al.*); layer 11 (sage-green silt), early Late Pleistocene, with abundant lithic and osseous technologies as well as faunal remains, associated with two incomplete human skulls (Z. Li, Wu, *et al.* 2017). The faunal assemblage from this last layer is mostly composed of *Equus caballus*, *Equus hemionus*, and *Bos primigenius* remains. Skeletal elements of *Megaloceros ordosianus*, *Cervus elaphus*, *Coelodonta antiquitatis*, *Procapra przewalskii*, *Dicerorhinus mercki*, *Pachycrocuta* cf. *sinensis*, *Palaeoloxodon* sp., *Viverra* cf. *zibetha*, *Ursus* sp., *Sus lydekkeri*, *Hydropotes pleistocenica*, and *Axis shansius lingjingensis* subsp. nov. were also identified (Dong & Li 2009; Li & Dong 2007). Hyena remains and coprolithes were found at the site (Z. Li & Dong 2007; Wenjuan Wang *et al.* 2014; 2015) but this specie played a marginal role in the accumulation of the faunal assemblage. The high proportion of limb bones (>60%), the high frequency of cut-marks (~34%), and their location on the bones suggest that Lingjing layer 11 was a kill-butchery site (Zhang *et al.* 2011; 2012).

OSL ages from layer 11 indicate a deposition taking place at *c.* 125 – 105 ka BP (Nian *et al.* 2009). This age situates the human occupation during the early phases of MIS5 (MIS5e to MIS5d). The lithic assemblage is mostly composed of quartz and

quartzite artefacts, and of sandstone and basalt in marginal proportions (H. Li *et al.*). The presence of cores, flakes, formal tools (i.e., scrapers, notches, denticulates, borers, points, choppers, etc.), debris, and the identification of use wear on some artefacts suggest that knapping activities, and tool manufacture and use occurred at the site (Li 2007). A few limb bone fragments and an antler bear traces indicating that they were used to retouch stone tools (Doyon *et al.* 2018). The two engraved bone fragments described in this study come from layer 11. They were discovered in 2009 (catalogue numbers 9L0141 and 9L0148) and identified by some of us (LZ, LH, LD, FD) as engraved during an analysis of the faunal assemblage conducted in 2016.

Online Supplementary Material 3: Materials and methods

SEM-EDS analysis of the red residue trapped in the lines on specimen 9L0141 was attempted with a JEOL JSM-6700F. Backscattered electron images (BSE) and elemental analyses were conducted under a low vacuum mode with an accelerating voltage of 3kV. BSE images were collected with a SiLi detector and EDS analyses with a SDD-EDAX detector. The analysis was interrupted for conservation before reliable EDS spectra could be acquired owing to the appearance of micro-cracks on the bone surface.

Raman analyses on specimen 9L0141 were conducted with an inVia Qotor confocal Raman Microscope (Renishaw) equipped with an internal calibration system. The analyses were done with a 785 nm laser and a power of 0.5% in order to avoid transformation of mineral phases. Acquisition time was set to 10s and multiple co-additions. The spectrometer worked in a spectral range from 100 to 1500 cm^{-1}. Five areas were analyzed, three with and two without red residue. Data was collected with the software package WIRE3. A sample of haematite curated at the Institute of Cultural Heritage, Shandong University, was also analysed following the same procedure. The mineral phase identification was based on the comparison of the recorded spectra with those of several spectra libraries (de Faria *et al.* 1997; Castro *et al.* 2005).

Sediment trapped in the spongy bone of specimen 9L0141 (OSM 8) was sampled under microscope, and analyzed with a JEOL JSM-6460LV SEM. The observations and analyses were conducted under a low vacuum mode by using an accelerating voltage of 20 kV. Element analyses were carried out with an EDS INCA Oxford 300 spectrometer. During the analyses, the working distance was kept constant (8 mm). Acquisition time was set up to 60 seconds for each EDS spectrum with an average downtime of 40%.
Two sediment samples were collected in 2016 from layer 11, west profile. ED-XRF analysis of these samples was carried out using a portable SPECTRO xSORT X-ray fluorescence spectrometer from AMETEK equipped with a silicon drift detector (SDD) and a low power W X-ray tube with an excitation source of 40 kV. Samples were positioned above a 7mm diameter spectrometer aperture and analysed from below for 60 seconds. For data treatment, we used the peak count rates of all detected elements and quantitative data for a selection of elements. The quantitative data were calculated according to a calibration operated with AMETEK X-LabPro software. This calibration was constructed by using 12 certified and local references and allows for the semi-

quantification of 7 major and trace elements among the most abundant in ferruginous rocks (normalised concentrations are presented in oxide weight).

Online Supplementary Material 4: Taphonomic analysis.

Table 2 Bone modifications recorded on Lingjing faunal remains analysed in this study.

	n	Non-human			Human			
		Root etching	Carnivore	Digestion	Cutmarks	Marrow extraction	Retouchers	Burnt bone
Total	227	50	9	5	54	8	7	3
Percentage	100%	22.03%	3.96%	2.20%	23.79%	3.52%	3.08%	1.32%

Table 3 Data on cut marks identified on Lingjing faunal remains

Catalogue n°	Number of cut marks	Arrangement	Morphology	Side striations	Changes in direction (*n*)	Edge morphology	Surface breaks (*n*)
7L036	15	Parallel	Straight	Yes	Yes (1)	Clean and Fringed	Yes (3)
6L1019	4	Parallel	Straight	Yes	No	Clean	No
5L004	2	Parallel	Curved	No	No	Clean	No
14L832a	7	Sub-parallel	Straight and Curved	No	No	Clean	No
14L832b	6	Divergent	Straight and Curved	Yes	No	Clean	No
5L858	2	Divergent	Straight and Curved	No	No	Clean	No
14L728	1	na	Straight	Yes	No	Clean	No
15L079	1	na	Straight	No	Yes (1)	Clean	No
6L1415a	6	Overlapping	Straight	Yes	No	Clean	Yes (1)
6L1415b	2	Divergent	Sinuous	No	Yes (2)	Clean	No
10L372	6	Sub-parallel	Straight	Yes	No	Clean	Yes (2)
9L0143	4	Parallel and Divergent	Straight	No	Yes (one has 3)	Clean	No
6L2544	2	Parallel	Sinuous and Curved	Yes	Yes (1)	Clean	No
8L0500	2	Parallel	Straight	No	No	Clean	No
6L2050	8	Divergent	Curved	No	No	Clean	No
14L764	1	na	Sinuous	No	Yes (1)	Clean	No
6L2095	1	na	Straight	No	No	Clean	No
15L077	8	Parallel	Straight	No	No	Clean	No
5L571	2	Parallel	Curved	Yes	No	Clean	No
6L1997	8	Divergent	Straight and Curved	Yes	Yes (1)	Clean	No
6L2197	4	Sub-parallel	Straight and Curved	No	No	Clean	No
9L0094	8	Parallel	Straight	Yes	No	Clean	No
6L780	12	Sub-parallel	Straight	No	Yes (2 due to bone morphology)	Clean	No
6L2034	4	Divergent	Straight	No	Yes (1)	Clean	No
6L771	1	na	Straight	No	No	Clean	No
9L0148	10	Parallel	Straight	No	No	Clean	No

Online Supplementary Material 5: Morphometric and technological data on Lingjing engraved specimens.

Table 4 Morphometric and technological data on specimen 9L0141

Lines	Start line (before or after fracture)	End line (before or after fracture)	Morphology			Technology					
			Section	Shape	Line keeps a constant depth on concave and convex area	Internal striations	Side striations	Bone breaks	Change in direction	Presence of residue	Same tool
1	na	Before	Asymmetrical to the right	U with flat base	Yes	No	No	Yes (1)	Yes (4)	No	a
2	Before	Before	Asymmetrical to the right	U with flat base	Yes	No	Yes (left [single])	Yes (5)*	Yes (3)	Yes	a
3	na	na	Asymmetrical to the right	U with polygonal base	Yes	Yes	Yes (right [single]; left [single])	Yes (2)	Yes (4)	No	b
4	After	Before	Asymmetrical to the right	U with polygonal base	Yes	Yes	Yes (right [double]; left [single])	Yes (1)	Yes (7)	Yes	b
5	na	na	Asymmetrical to the right	U with flat base	Yes	Yes	Yes (right [double]; left [single])	Yes (1)	Yes (5)	Yes	b
6a	na	na	na	na	Too superficial	na	na	No	No	No	na
6b	na	na	Symmetrical	U	Too superficial	Yes	No	No	Yes (3)	Yes	b
6c	na	na	Asymmetrical to the right	U with polygonal base	Too superficial	Yes	No	No	Yes (2)	Yes	b
7a	na	na	na	na	Too superficial	na	No	No	No	No	na
7b	na	na	Asymmetrical to the right	U with polygonal base	Yes	Yes	No	No	No	No	b
7c	na	na	na	na	Too superficial	na	No	No	No	No	na
7d	na	na	Asymmetrical to the right	U with polygonal base	Yes	Yes	No	No	No	No	b
7e	na	na	na	na	Too superficial	na	No	No	No	No	na

Table 5 Morphometric and technological data on specimen 9L0148

Lines	Start line (before or after fracture)	End line (before or after fracture)	Morphology		Technology					
			Section	Shape	Internal striations	Side striations	Bone breaks	Change in direction	Presence of residue	Same tool
1	Before	Before	Asymmetrical to the right	Polygonal	Yes	No		No	No	a
2	Before	Before	Asymmetrical to the right	Polygonal	Yes	No		No	No	a
3	Before	na	Asymmetrical to the right	Polygonal	Yes	No		No	No	a
4	Before	na	Asymmetrical to the right	Polygonal	Yes	No		No	No	a
5	Before	Before	Asymmetrical to the right	Polygonal	Yes	No	Yes	No	No	a
6	Before	na	Asymmetrical to the right	Polygonal	Yes	No		No	No	a
7	Before	na	Symmetrical	Polygonal	Yes	No	Yes	No	No	a
8	Before	Before	Symmetrical	Polygonal	Yes	No	Yes	No	No	a
9	Before	na	Symmetrical	Polygonal	Yes	No		No	No	a
10	Before	na	Symmetrical	Polygonal	Yes	No	Yes	No	No	a

Online Supplementary Material 6: Microscopic analysis of specimen 9L0141.

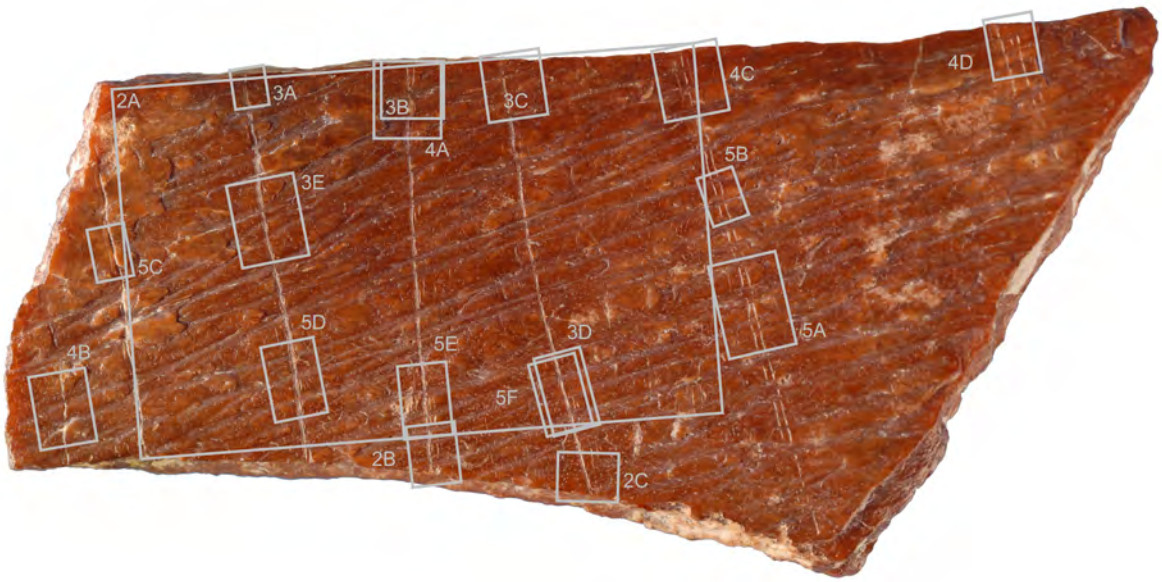

Figure 1 Location of the microscopic photographs present in OSM 6, Figures 2-5.

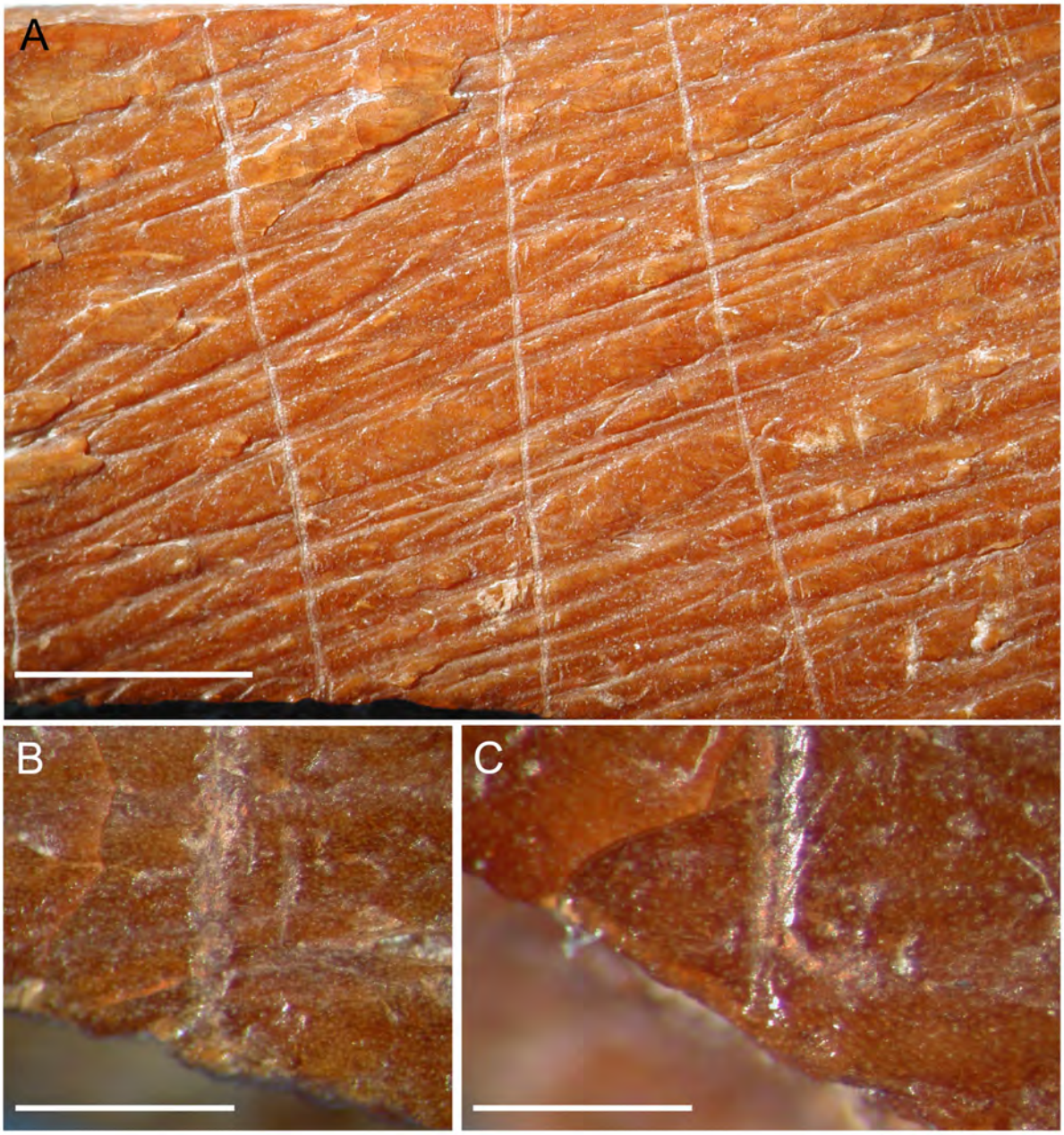

Figure 2 (A) Periosteal surface of specimen 9L0141 showing a rugged fibrous structure. Lower termination of lines (B) L4 and (C) L5 showing they were interrupted by the fracture of the bone. Scales: (A) = 5mm; (B-C) = 500µm.

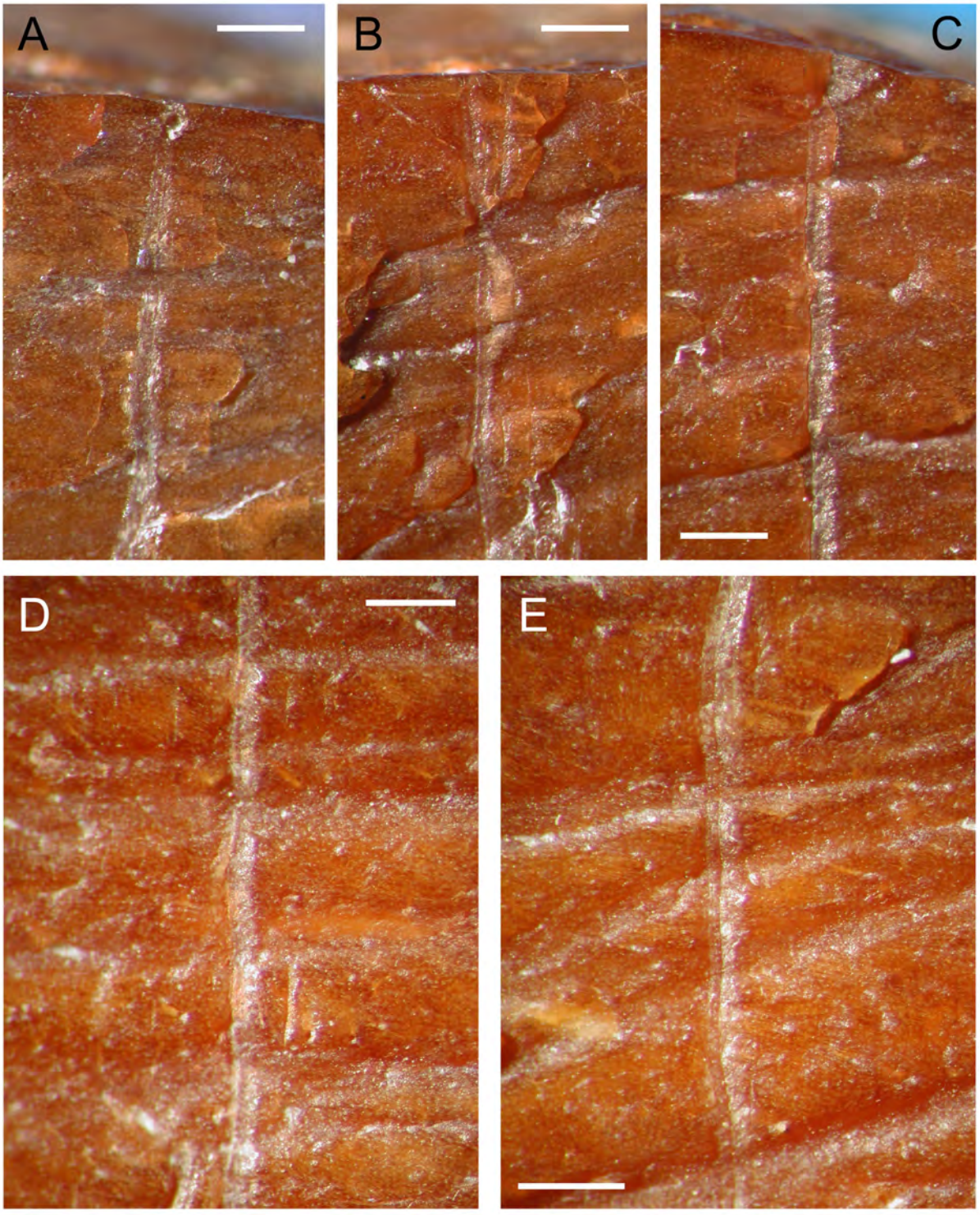

Figure 3 Upper termination of lines (A) L3, (B) L4, and (C) L5 showing they were engraved after the fracture of the bone. Notice (D) the grainy appearance of the line's surface and (E) the micro-fringed outlines. Scales: (A-E) = 500µm.

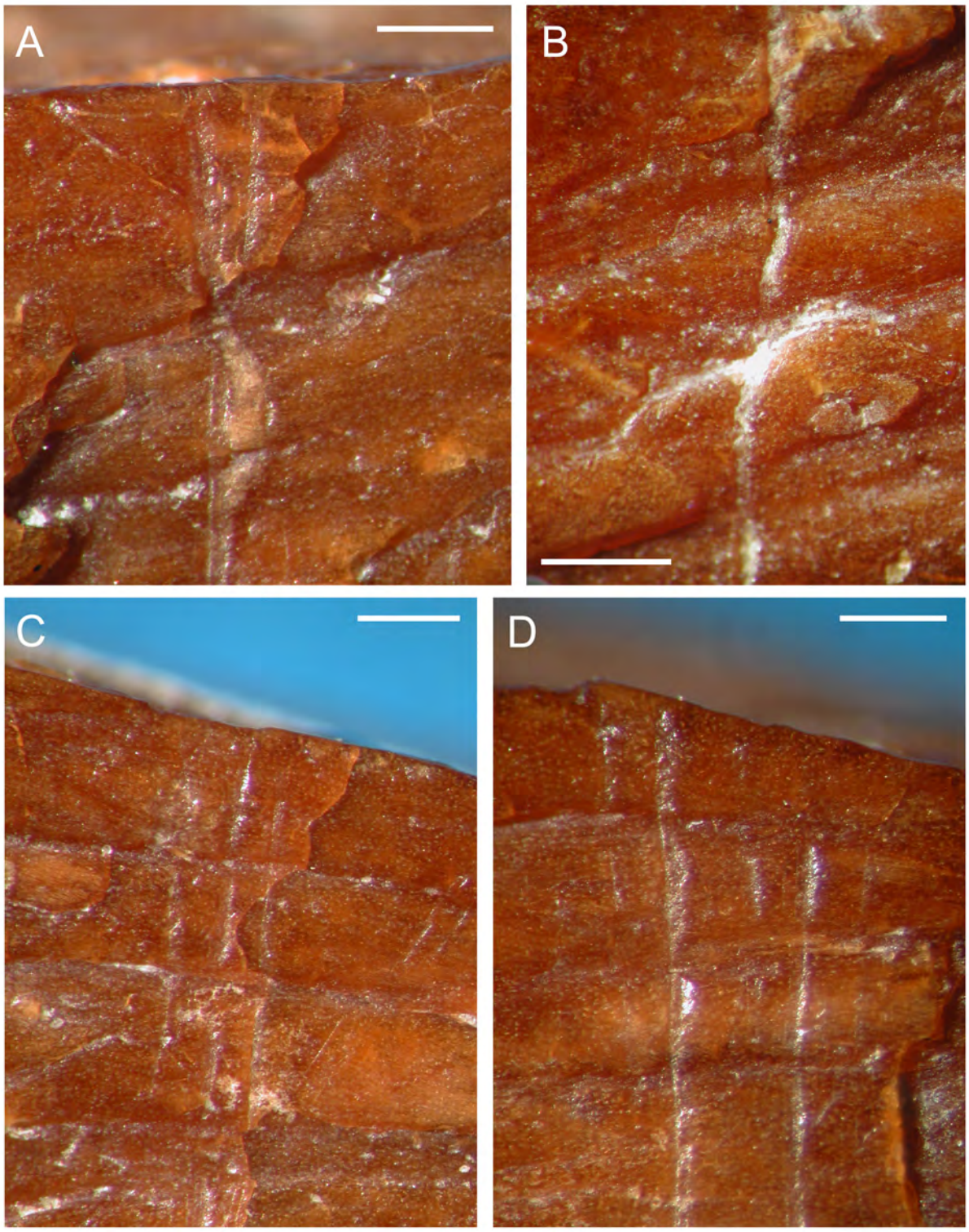

Figure 4 Close-up view of lines (A) L4, (B) L1, (C) L6, and (D) L7. Notice (A) the step micro-fractures occurring when the line crosses natural ridges. (B) Changes in direction of the line and micro-fractures produced when crossing the ridge indicate the direction of the motion. Scales: (A-D) = 500µm.

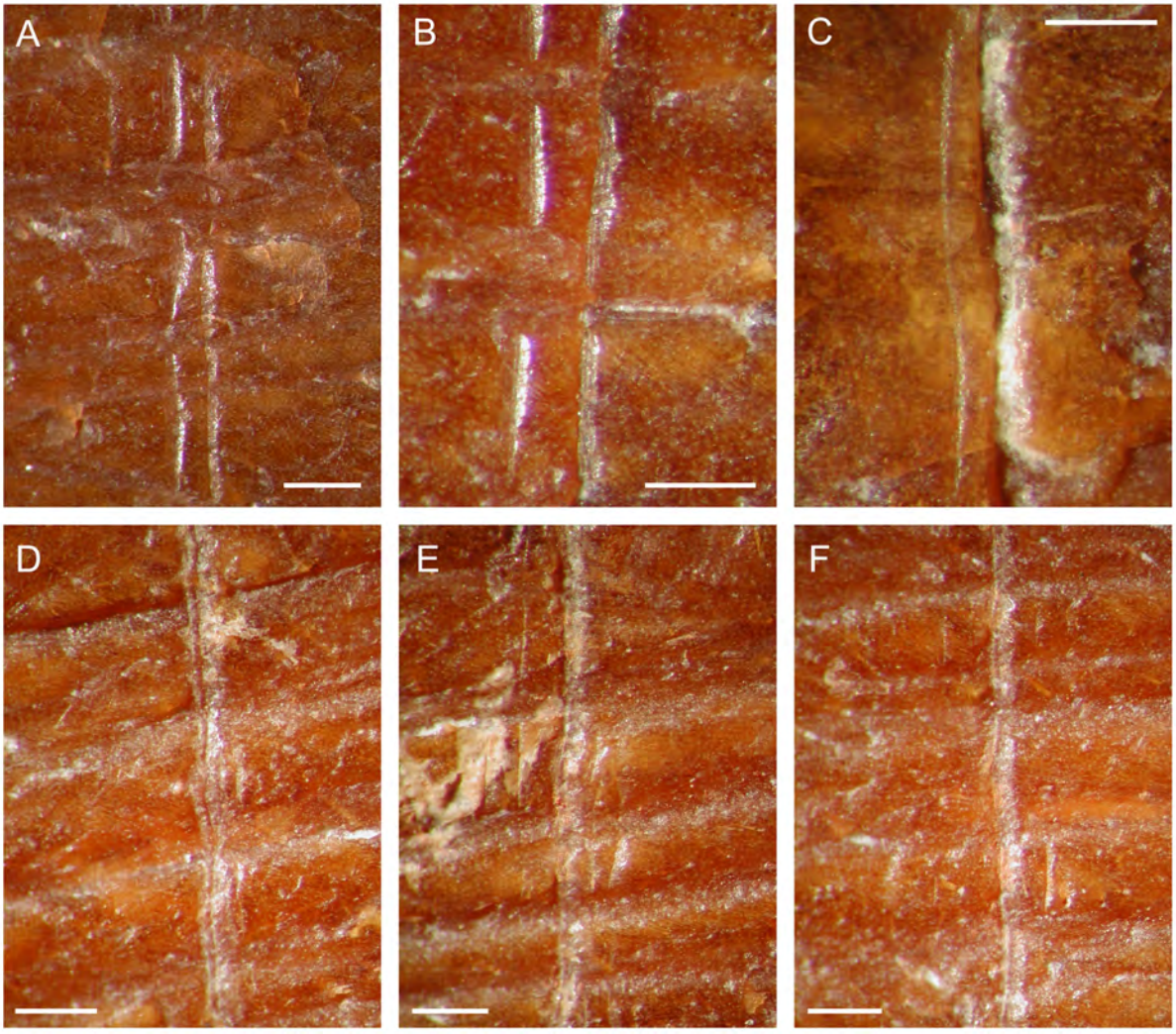

Figure 5 Close-up view of lines (A-B) L6, (C) L2, (D) L3, (E) L4, and (E) L5 on specimen 9L0141. Notice changes in direction (A-B) indicating the line was engraved my multiple strokes using the same tool (B). Side striations (C-F) result from the discontinuous contact of protuberances on the tool tip. Scales: (A-F) = 500µm.

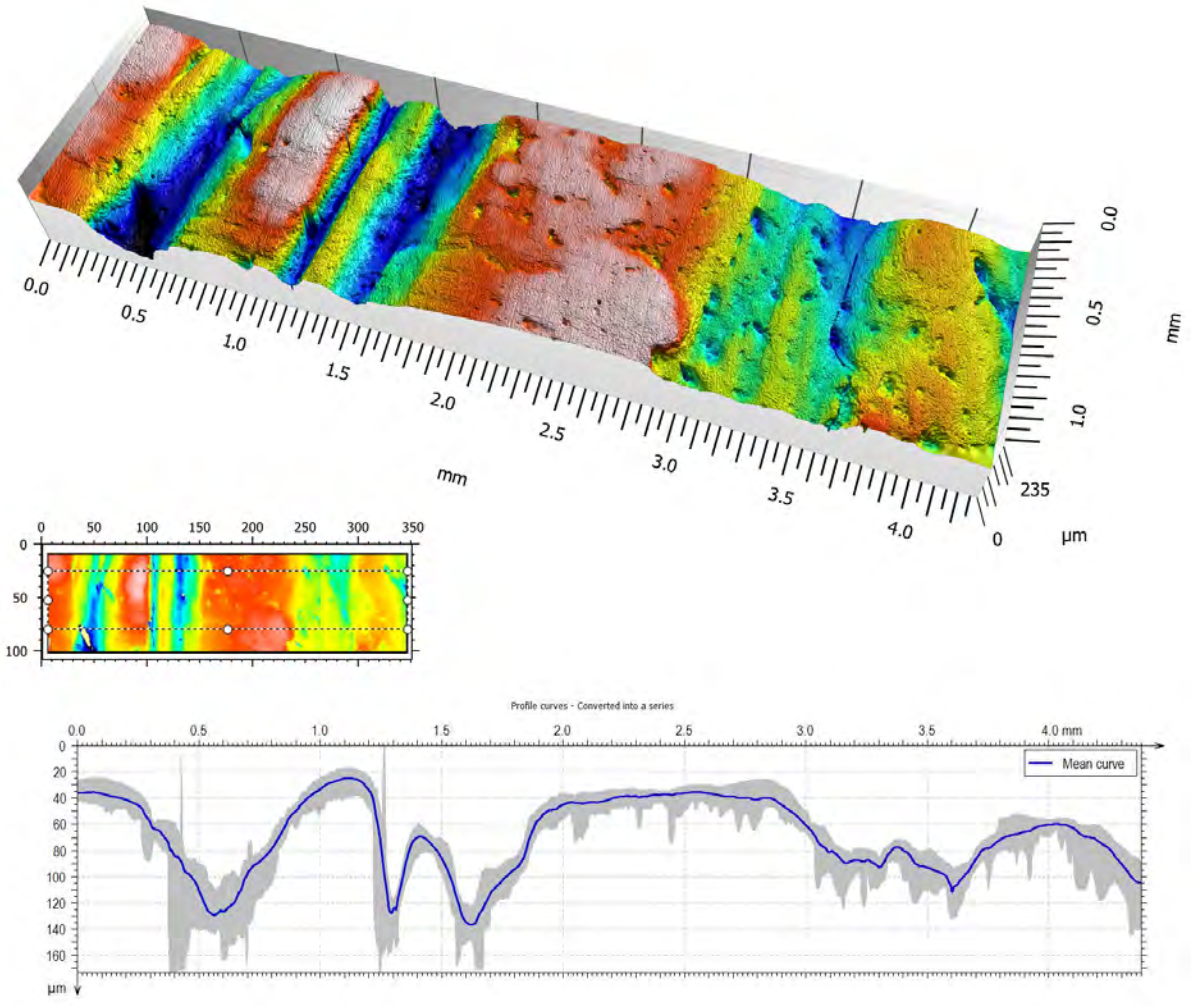

Figure 6 3D rendering of a selected area of the bone periosteal surface on specimen 9L0141 (top) showing its rugged morphology; (bottom) mean profile curve (blue) of the area indicated in the sketch (centre). Grey surface summarizes depth variation.

Online Supplementary Material 7: Residue and sediment analysis.

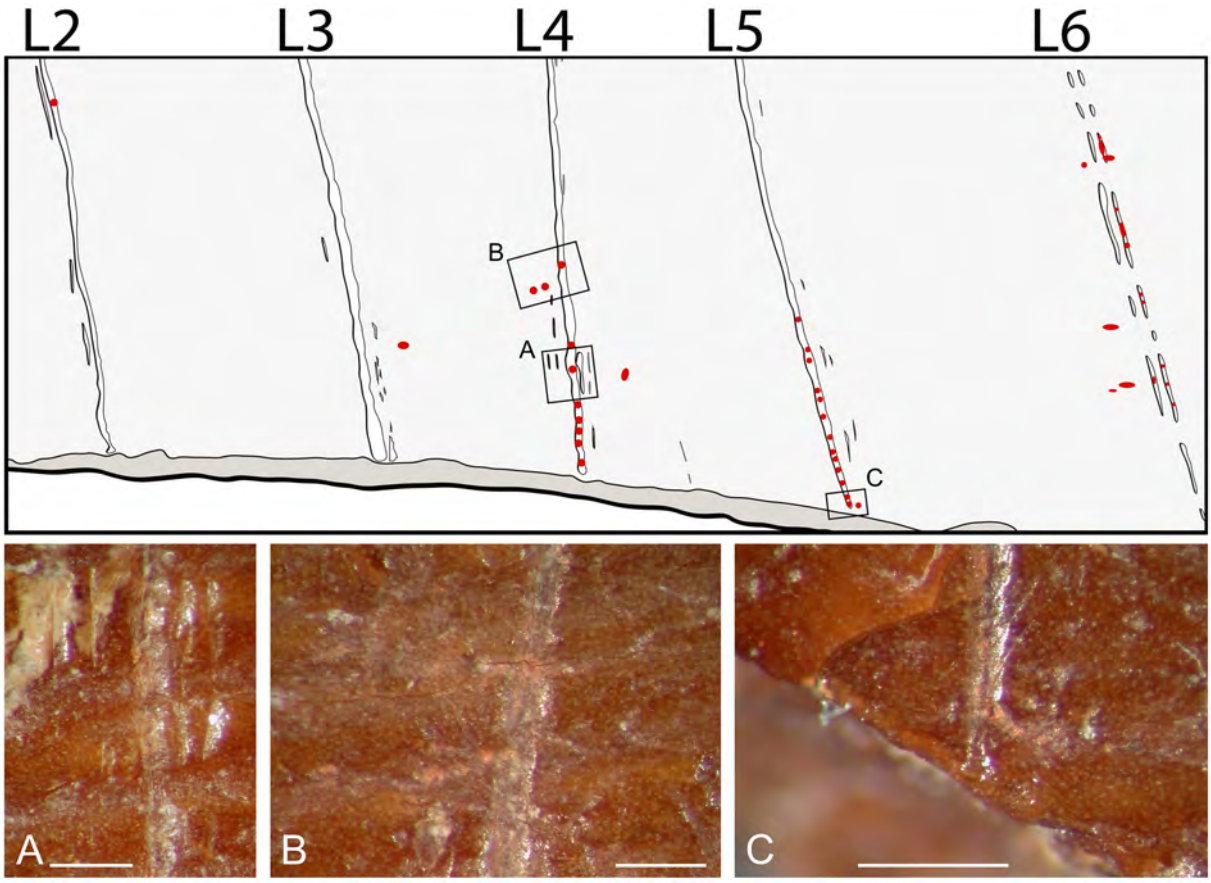

Figure 7 Location of red residues on specimen 9L0141 (top), and close-up view of residues on lines (A-B) L4, (C) L5. Scales: (A-C) = 500µm.

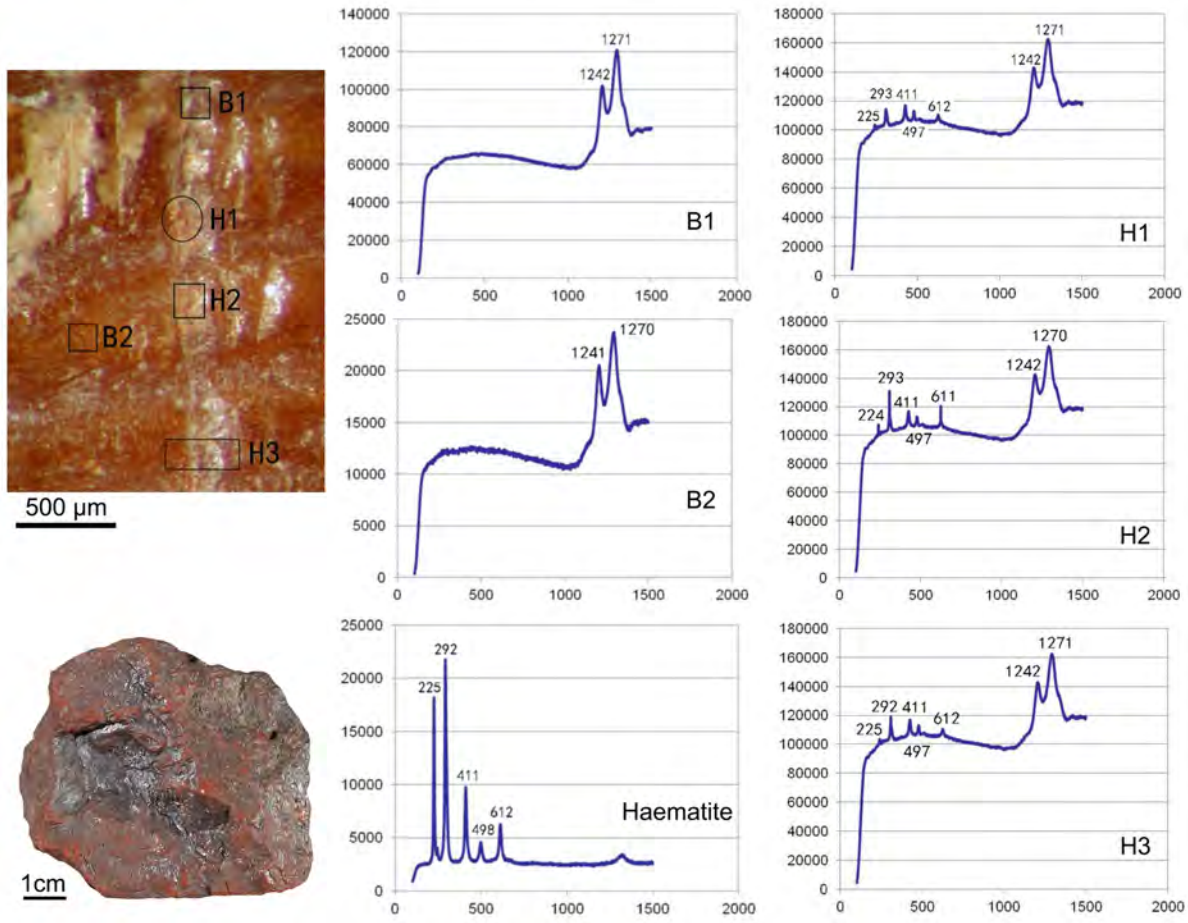

Figure 8 Location of Raman analyses (top left) on specimen 9L0141. B1-B2: bone surface; H1-H3: red residues. Haematite fragment curated at the Institute of Cultural Heritage, Shandong University, used for comparison (bottom left), and Raman spectra obtained from analysed spots (right).

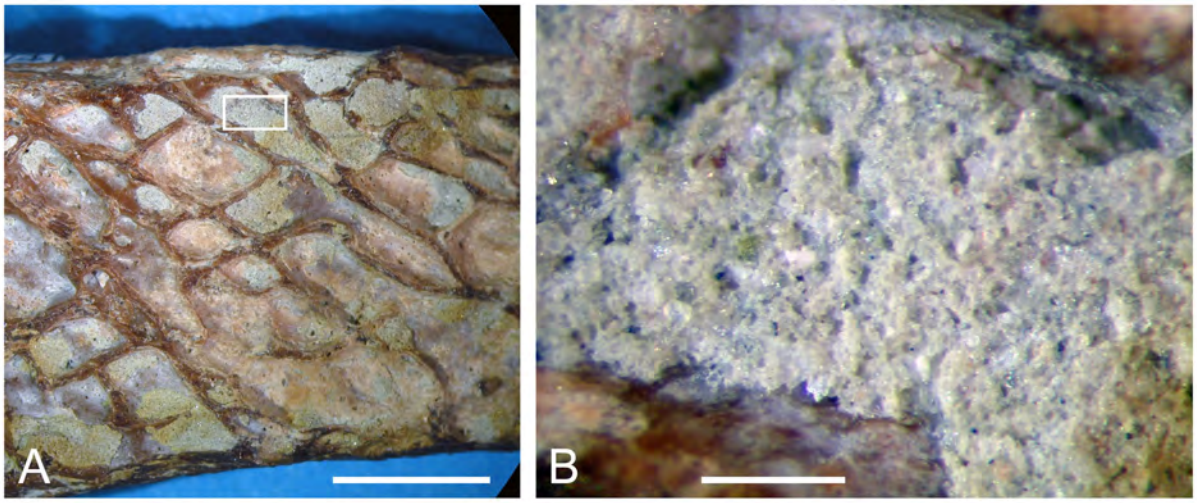

Figure 9 Endosteal surface of specimen 9L0141 with spongy bone (A) filled with sediment (B) from layer 11. Notice the whitish colour of the sediment and the absence of red particles. Scales: (A) = 5mm; (B) = 500µm.

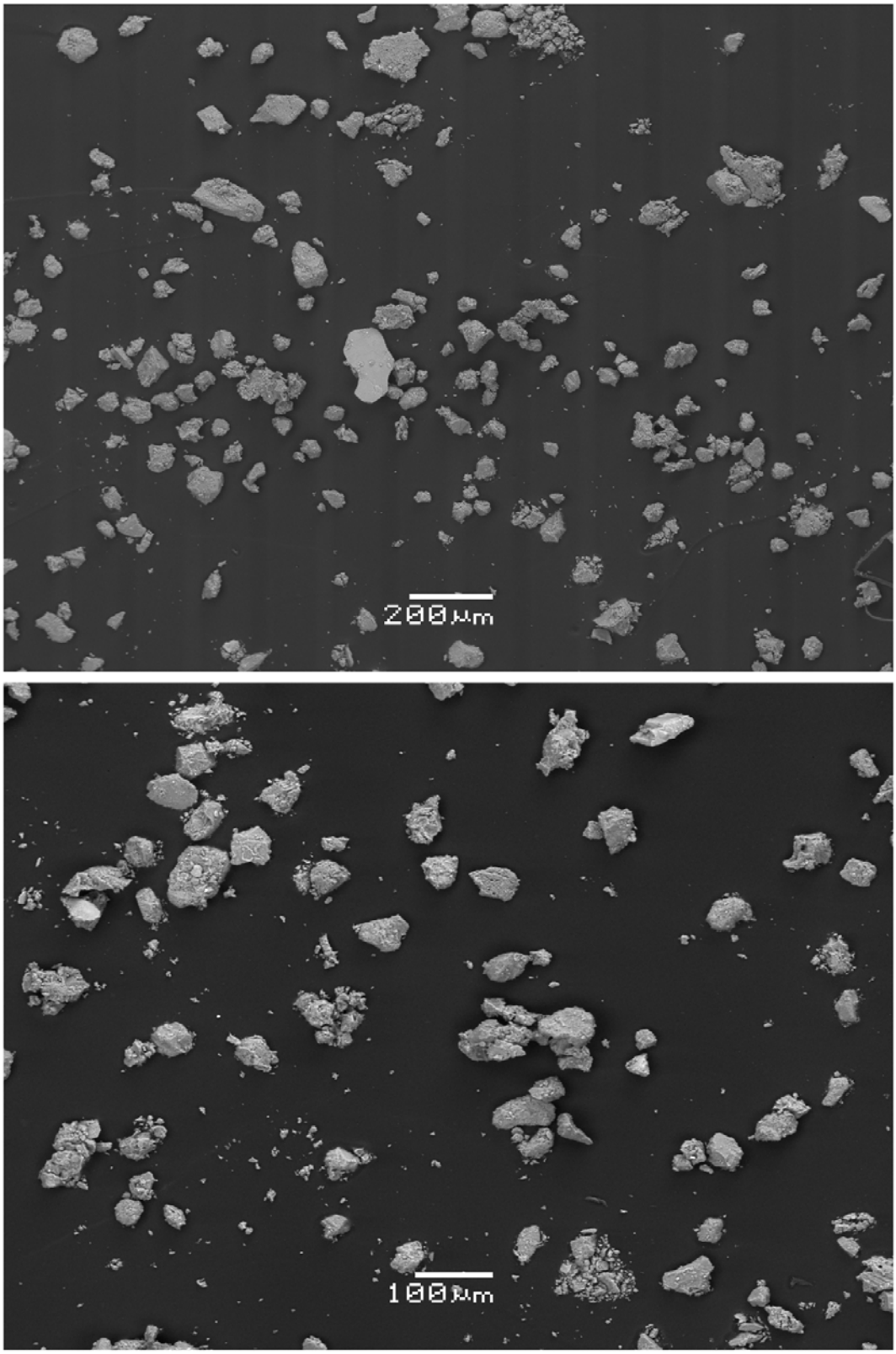

Figure 10 SEM photographs in backscattered mode of particles composing the sediment sampled from the spongy bone of specimen 9L0141.

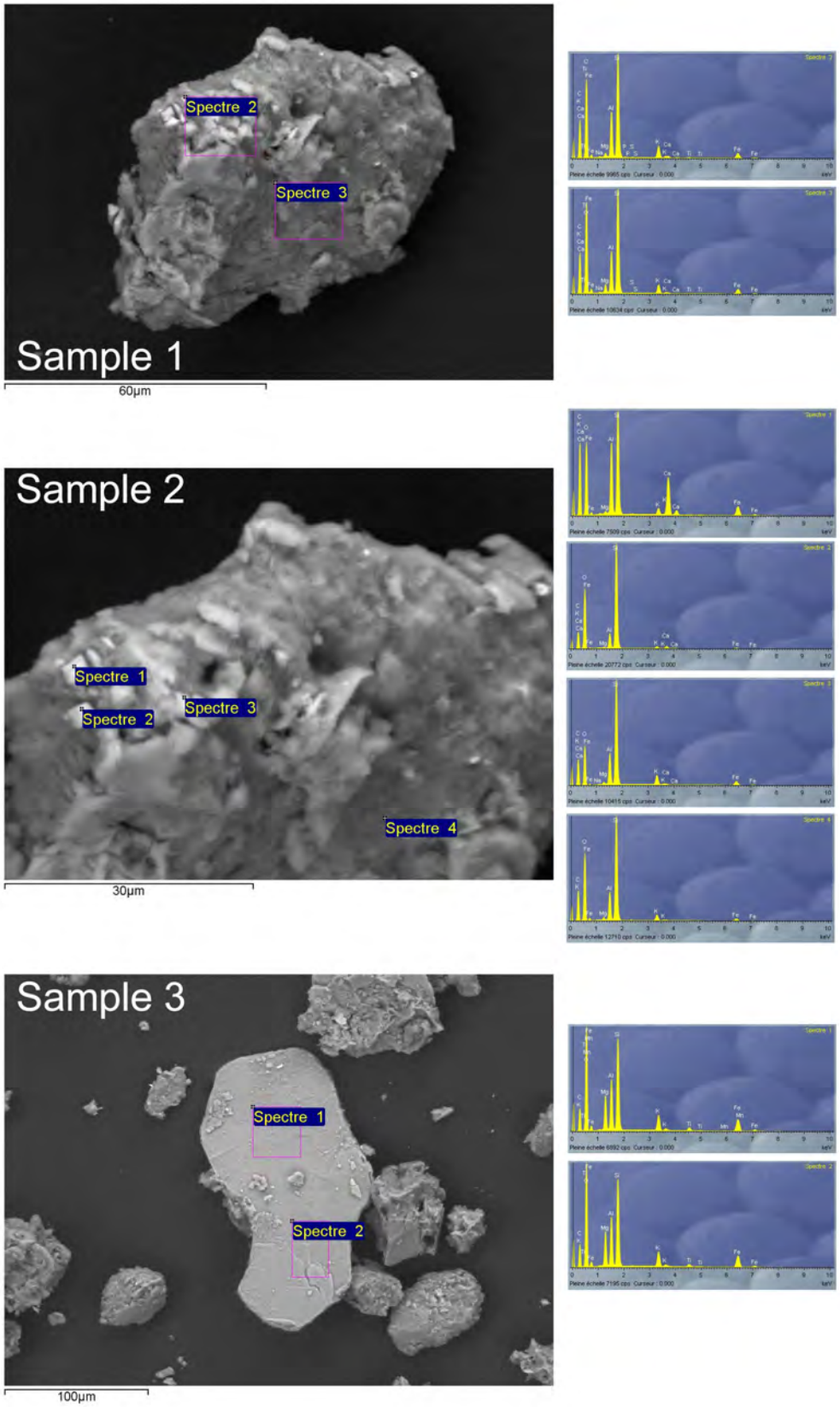

Figure 11 SEM-EDS analyses of sediment particles (sample 1-3) sampled from the spongy bone of specimen 9L0141. Table 6 for detailed results.

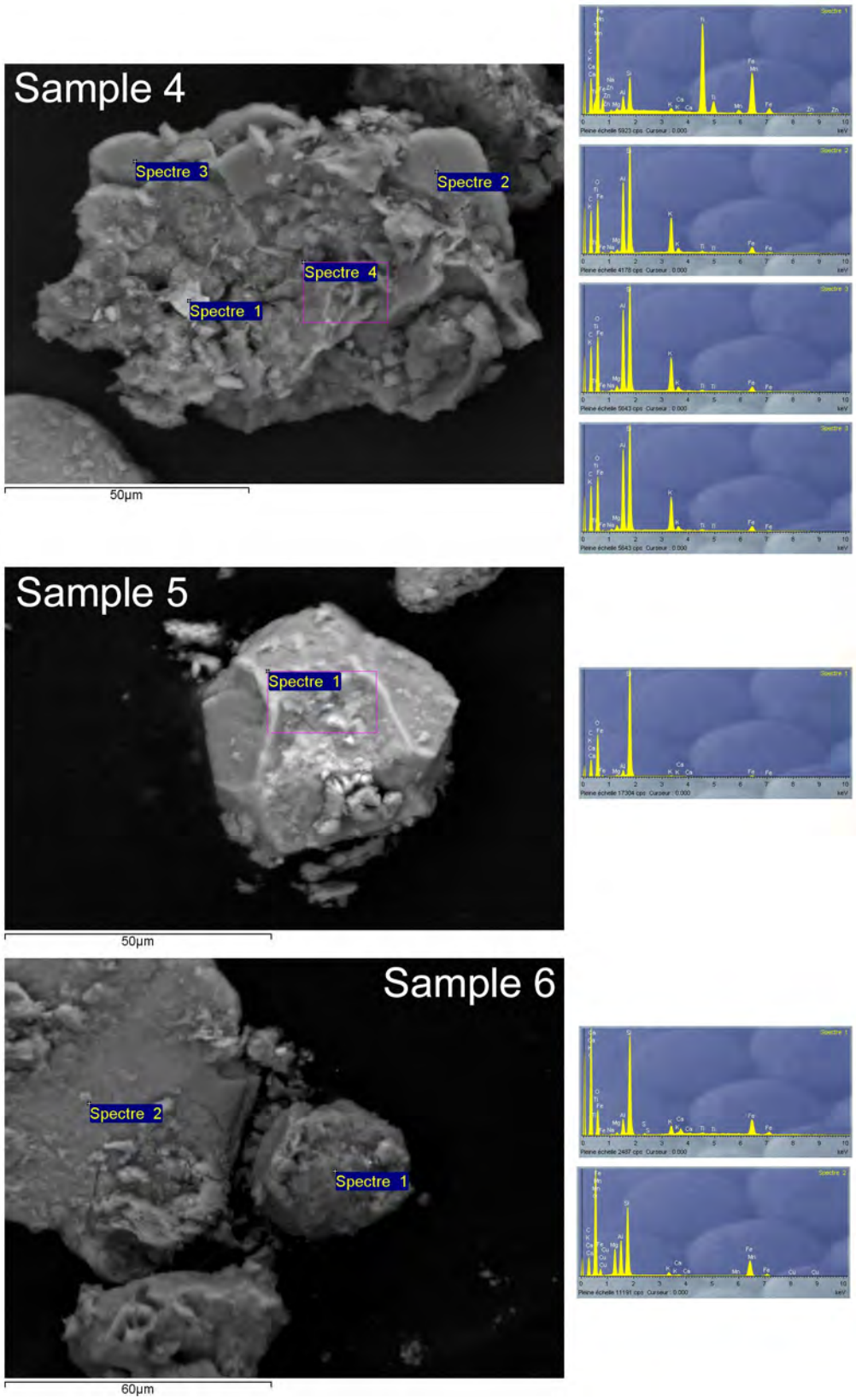

Figure 12 SEM-EDS analyses of sediment particles (sample 4-6) sampled from the spongy bone of specimen 9L0141. Table 6 for detailed results.

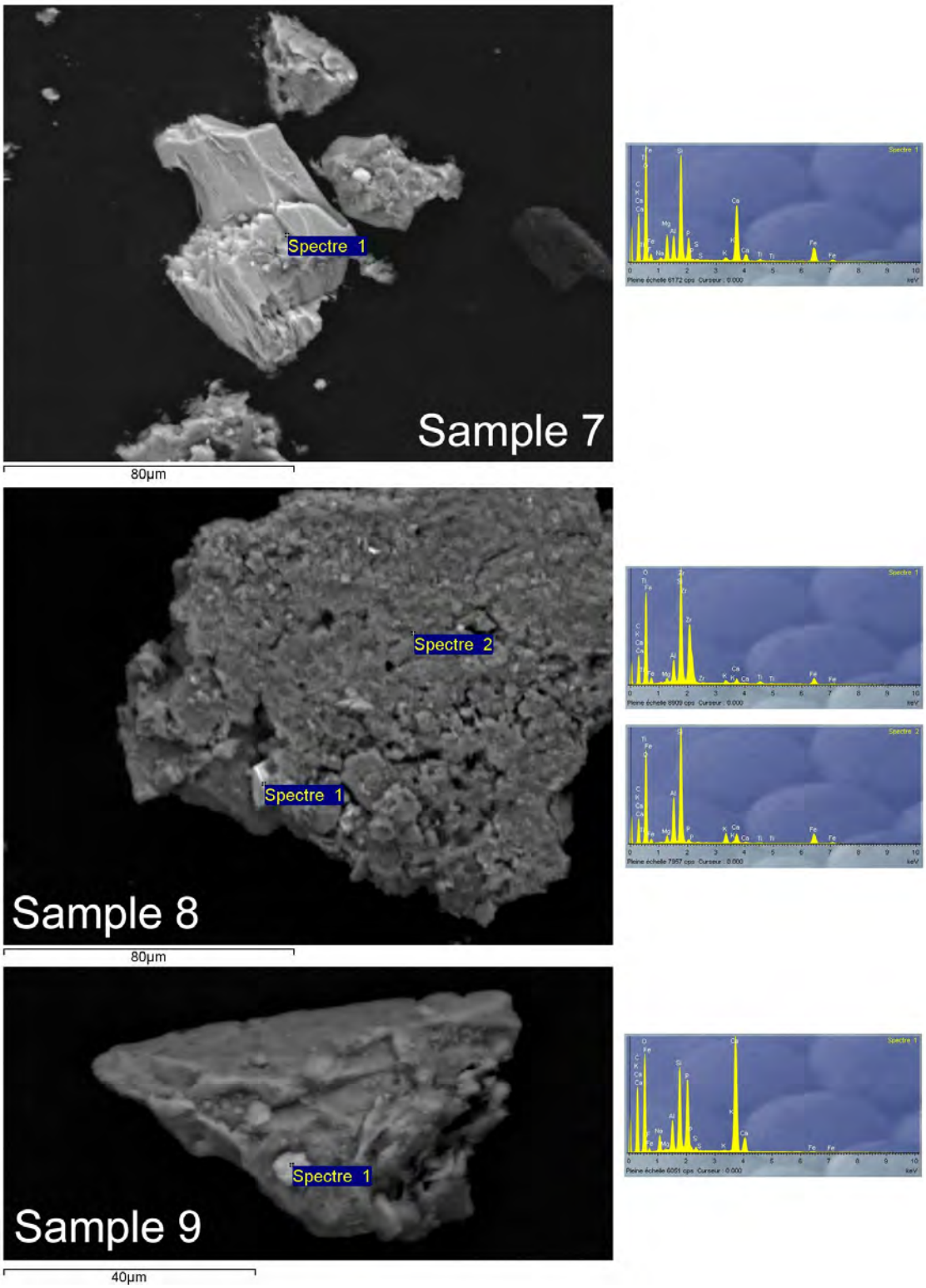

Figure 13 SEM-EDS analyses of sediment particles (sample 7-9) sampled from the spongy bone of specimen 9L0141. Table 6 for detailed results.

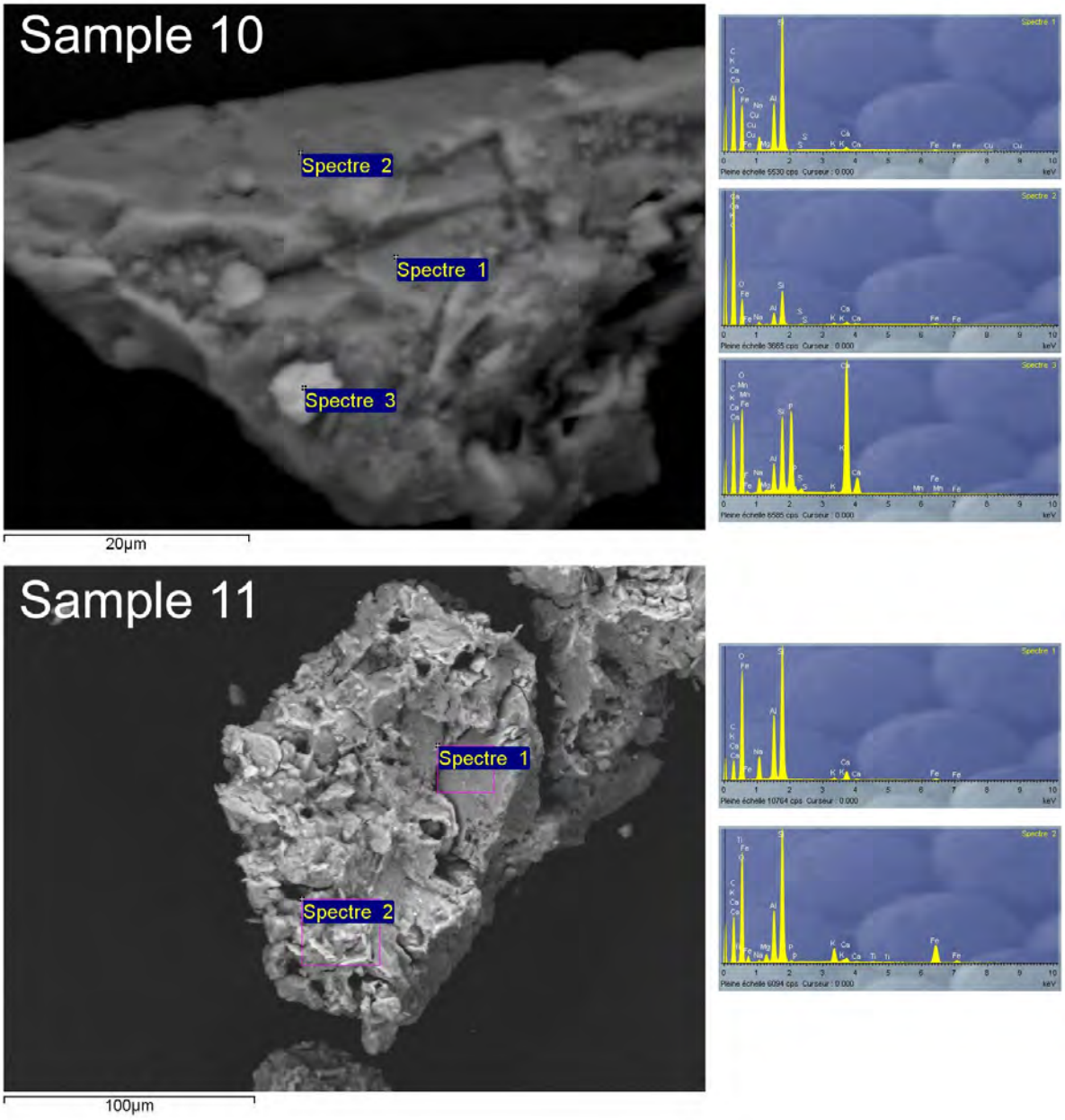

Figure 14 SEM-EDS analyses of sediment particles (sample 10-11) sampled from the spongy bone of specimen 9L0141. Table 6 for detailed results.

Table 6 Proportion of chemical elements detected by SEM-EDS on the sediment sampled from the spongy bone of specimen 9L0141.

Sample	Zone	Type	Na_2O	MgO	Al_2O_3	SiO_2	P_2O_5	K_2O	CaO	TiO_2	MnO	Fe_2O_3	CuO	ZnO	ZrO_2	Total
1	2	Clay	0.4	1.9	**20.7**	**58.4**	0.5	6.1	1.2	0.6	0.0	10.1	0.0	0.0	0.0	99.9
1	3	Clay	0.3	4.3	19.5	**60.5**	0.0	4.7	0.6	0.3	0.0	9.3	0.3	0.0	0.0	99.8
2	1	Clay	0.3	0.8	**23.6**	**42.8**	0.0	2.4	17.8	0.0	0.0	12.2	0.0	0.0	0.0	99.9
2	2	Clay	0.2	0.6	9.4	**83.0**	0.0	1.8	2.6	0.0	0.0	2.5	0.0	0.0	0.0	100.0
2	3	Clay	0.3	1.3	16.2	**66.5**	0.0	5.8	0.5	0.3	0.0	8.6	0.4	0.0	0.0	99.9
2	4	Clay	0.2	1.6	15.8	**72.6**	0.0	3.9	0.4	0.2	0.0	5.2	0.0	0.0	0.0	99.9
3	1	Clay	0.0	13.5	19.4	**41.6**	0.0	5.8	0.3	2.5	0.3	16.6	0.0	0.0	0.0	100.0
3	2	Clay	0.0	13.8	19.6	**41.1**	0.0	5.8	0.3	2.4	0.2	16.8	0.0	0.0	0.0	99.9
4	1	Iron	0.4	0.8	4.0	9.6	0.0	0.8	0.3	**45.5**	2.2	**35.6**	0.0	0.9	0.0	100.0
4	2	Clay	0.7	1.0	**25.2**	**48.3**	0.0	14.4	0.4	1.4	0.0	8.7	0.0	0.0	0.0	100.0
4	3	Clay	0.5	1.7	**28.1**	**47.9**	0.0	13.2	0.4	0.8	0.0	7.3	0.0	0.0	0.0	100.0
4	4	Clay	0.4	3.3	**21.9**	**55.6**	0.7	4.9	1.5	1.1	0.0	10.7	0.0	0.0	0.0	99.9
5	1	Quartz	0.2	0.8	4.1	**90.3**	0.0	0.9	0.3	0.0	0.0	3.4	0.0	0.0	0.0	99.9
6	1	Clay	0.5	1.3	7.6	**53.7**	0.0	4.3	3.0	0.9	0.0	**27.0**	1.2	0.0	0.0	99.6
6	2	Clay	0.0	14.1	17.8	**40.1**	0.0	1.3	0.4	0.0	0.3	**25.9**	0.3	0.0	0.0	100.0
7	1	Clay	0.7	8.0	7.1	**33.4**	11.8	1.0	**20.5**	1.3	0.3	15.7	0.0	0.0	0.0	99.8
8	1	Zircon	0.0	1.4	6.4	**35.5**	0.0	1.3	1.8	1.7	0.0	7.4	0.0	0.0	**44.6**	100.0
8	2	Clay	0.2	2.9	17.0	**52.8**	3.0	3.9	4.7	0.6	0.0	14.9	0.0	0.0	0.0	99.9
9	1	Bone	4.1	0.4	6.8	**20.9**	**28.5**	0.3	**37.2**	0.0	0.3	0.7	0.4	0.0	0.0	99.5
10	1	Clay	6.1	0.3	19.6	**69.5**	0.0	0.6	2.0	0.0	0.0	1.0	0.7	0.0	0.0	99.8
10	2	Clay	4.6	0.0	17.4	**62.3**	0.0	3.1	5.3	0.0	0.0	6.1	0.0	0.0	0.0	98.7
10	3	Bone	3.5	0.3	6.0	17.6	**30.6**	0.3	**39.8**	0.0	0.4	0.8	0.3	0.0	0.0	99.5
11	1	Clay	8.6	0.2	**22.9**	**60.5**	0.0	0.7	4.3	0.0	0.0	2.5	0.3	0.0	0.0	100.0
11	2	Clay	0.6	2.6	16.5	**50.8**	0.8	4.5	1.7	0.8	0.0	**21.7**	0.0	0.0	0.0	100.0

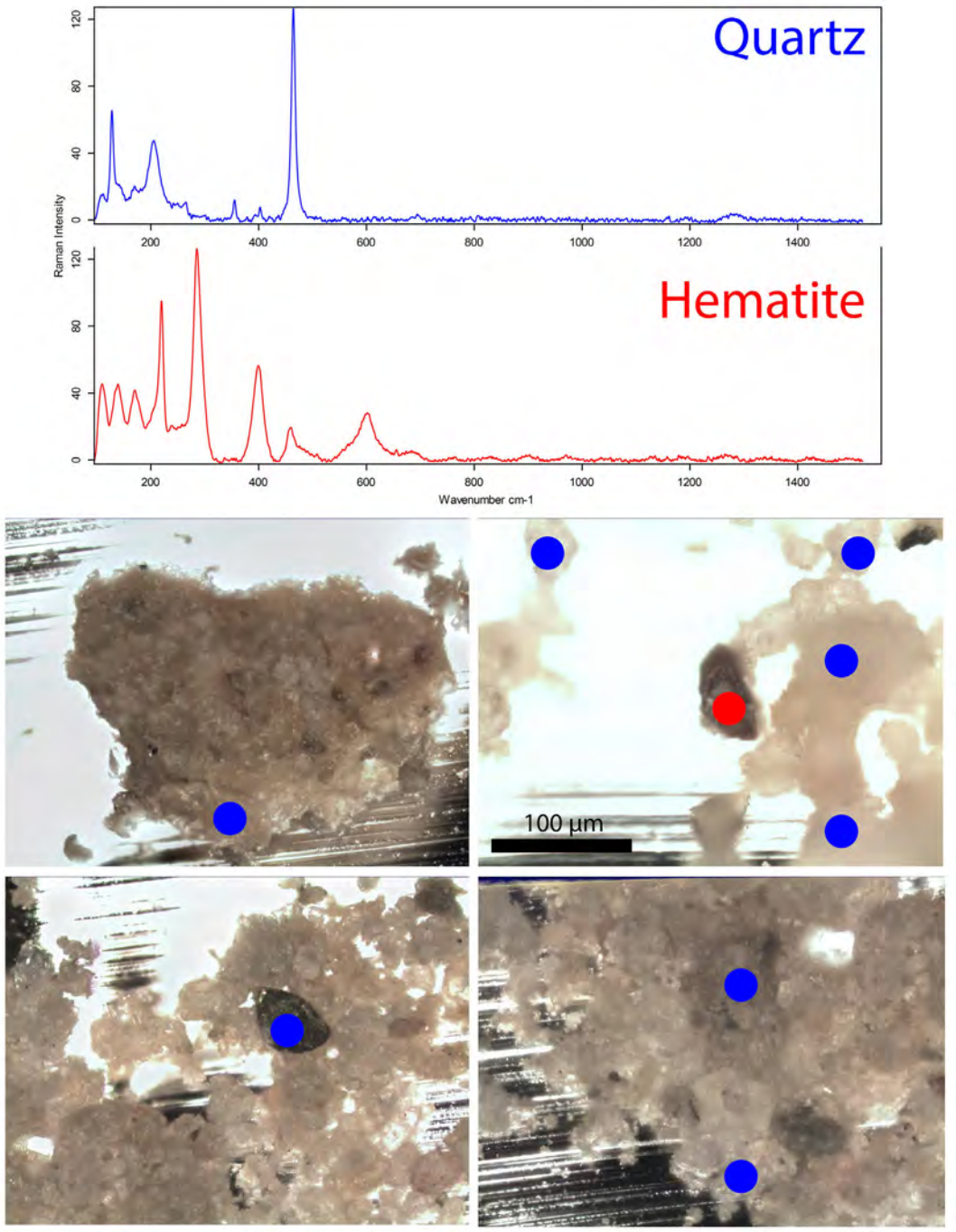

Figure 10 Raman spectra (top) for quartz (blue) and haematite (red) obtained when analysing dark particles in sediment from Lingjing, layer 11 (bottom).

Table 7 Elemental composition of sediment from Lingjing, layer 11 (ED-XRF).

Element	Si	K	Ca	Ti	V	Cr	Mn	Fe	Ni	Zn	Ga	As	Rb	Sr	Y	Zr	Ba	Pb	Th
Dimension	%	%	%	%	µg/g	µg/g	%	%	µg/g	µg/g	µg/g	µg/g	µg/g	µg/g	µg/g	µg/g	µg/g	µg/g	µg/g
Lingjing (Dry Sediment)	33.17	2.007	0.6343	0.3526	< 2,4	41.7	0.05517	2.599	20.1	36.1	14.2	8.4	150.5	135.3	32.9	358.6	555	9.9	11.9
Lingjing (Wet Sediment)	33.19	1.865	0.6206	0.3652	< 2,4	29	0.02451	2.4	19.9	44.4	13.9	10.6	126	170.2	26.8	315.4	515	8.7	7.8

References

BAHN, P.G. & J. VERTUT. 1997. *Journey through the Ice Age*. Los Angeles: University of California Press.

BORZATTI VON LÖWENSTERN, E. & D. MAGALDI. 1967. Ultime ricerche nella Grotta dell'Alto (S. Caterina, Lecce). *Rivista di scienze preistoriche* 22: 205–250.

BOURDIER, F. 1967. *Préhistoire de France*. Paris: Flammarion.

BUGGIANI, S., L. SARTI & F. MARTINI. 2004. Incisioni musteriane su pietra da Grotta del Cavallo (Lecce): contributo al dibattio sulle esperienze grafiche neandertaliane. *Rivista di scienze preistoriche*: 271–290.

CAIN, C.R. 2004. Notched, flaked and ground bone artefacts from Middle Stone Age and Iron Age layers of Sibudu Cave, KwaZulu-Natal, South Africa. *South African Journal of Science* 100: 195–197.

CAPITAN, L. & D. PEYRONY. 1912. La station préhistorique de la Ferrassie. *Revue Anthropologique* 22: 76–99.

CASTRO, K., M. PÉREZ-ALONSO, M.D. RODRÍGUEZ-LASO, L.A. FERNÁNDEZ & J.M. MADARIAGA. 2005. On-line FT-Raman and dispersive Raman spectra database of artists' materials (e-VISART database). *Analytical and Bioanalytical Chemistry* 382: 248–258.

CHEN, C. 1983. Preliminary exploration of the typology and technology of microcore in China - also of the culture relationship between Northeast Aria and Northwestern North America. *Acta Anthropologica Sinica* 2: 331–346.

CRÉMADES, M., H. LAVILLE, N. SIRAKOV & J. KOZLOWSKI. 1995. Une pierre gravée de 50 000 ans B.P. dans les Balkans. *Paléo* 7: 201–209.

D'ERRICO, F., L. BACKWELL, P. VILLA, I. DEGANO, J.J. LUCEJKO, M.K. BAMFORD, T.F.G. HIGHAM, M.P. COLOMBINI & P.B. BEAUMONT. 2012. Early evidence of San material culture represented by organic artifacts from Border Cave, South Africa. *Proceedings of the National Academy of Sciences* 109: 13214–13219.

D'ERRICO, F., L. DOYON, I. COLAGÉ, A. QUEFFELEC, E. LE VRAUX, G. GIACOBINI, B. VANDERMEERSCH & B. MAUREILLE. 2018. From number sense to number symbols: an archaeological perspective. *Philosophical Transactions of the Royal Society B* 373: 20160518.

D'ERRICO, F., R. GARCÍA MORENO & R.F. RIFKIN. 2012. Technological, elemental and colorimetric analysis of an engraved ochre fragment from the Middle Stone Age levels of Klasies River Cave 1, South Africa. *Journal of Archaeological Science* 39: 942–952.

D'ERRICO, F., C. HENSHILWOOD, G. LAWSON, M. VANHAEREN, A.-M. TILLIER, M. SORESSI, F. BRESSON, B. MAUREILLE, A. NOWELL, J. LAKARRA, L. BACKWELL & M. JULIEN. 2003. Archaeological evidence for the emergence of language, symbolism, and music: an alternative multidisciplinary perspective. *Journal of World Prehistory* 17: 1–70.

D'ERRICO, F., M. JULIEN, D. LIOLIOS, M. VANHAEREN & D. BAFFIER. 2003. Many awls in our argument: bone tool manufacture and use in the Châtelperronian and Aurignacian levels of the Grotte du Renne at Arcy-sur-Cure, in J. Zilhao & F. d'Errico (ed.) *The chronology of the Aurignacian and of the transitional technocomplexes: dating, stratigraphies, cultural implications*: 247–270. Lisbon: Instituto Português de Arqueologia.

D'ERRICO, F., M. VANHAEREN, C.S. HENSHILWOOD, G. LAWSON, B. MAUREILLE, D. GAMBIER, A.-M. TILLIER, M. SORESSI & K.L. VAN NIEKERK. 2009. From the origin of language to the diversification of languages: what can archaeology and palaeoanthropology say?, in F. d'Errico & J.-M. Hombert (ed.) *Becoming eloquent: advances in the emergence of*

language, human cognition, and modern cultures: 13–68. Amsterdam: John Benjamins Publishing Company.

D'ERRICO, F., J. ZILHÃO, M. JULIEN, D. BAFFIER & J. PELEGRIN. 1998. Neanderthal acculturation in Western Europe? A critical review of the evidence and its interpretation. *Current Anthropology* 39: S1–S44.

DE FARIA, D.L.A., S. VENÂNCIO SILVA & M.T. DE OLIVEIRA. 1997. Raman microspectroscopy of some iron oxides and oxyhydroxides. *Journal of Raman Spectroscopy* 28: 873–878.

DONG, W. & Z. LI. 2009. New cervids (Artiodactyla, Mammalia) from the Late Pleistocene of Lingjing Site in Henan Province, China. *Acta Anthropologica Sinica* 28: 319–326.

DOYON, L., Z. LI, H. LI & F. D'ERRICO. 2018. Discovery of *circa* 115,000-year-old bone retouchers at Lingjing, Henan, China. *PLOS ONE* 13: e0194318.

FRAYER, D.W., J. ORSCHIEDT, J. COOK, M.D. RUSSELL & J. RADOVČIĆ. 2006. Krapina 3: cut marks and ritual behavior? *Periodicum Biologorum* 108: 519–524.

GAO, X., W. HUANG., Z. XU., Z. MA. & J.W. OLSEN. 2004. 120–150 ka human tooth and ivory engravings from Xinglongdong Cave, Three Gorges Region, South China *Chinese Science Bulletin* 49: 175–180.

GARCÍA-DIEZ, M., B.O. FRAILE & I.B. MAESTU. 2013. Neanderthal graphic behavior: the pecked pebble from Axlor rockshelter (Northern Spain). *Journal of Anthropological Research* 69: 397–410.

GOREN-INBAR, N. 1990. *Quneitra: a Mousterian site on the Golan Heights. Vol. 31*. Qedem: Hebrew University of Jerusalem.

HENSHILWOOD, C.S., F. D'ERRICO & I. WATTS. 2009. Engraved ochres from the Middle Stone Age levels at Blombos Cave, South Africa. *Journal of Human Evolution* 57: 27–47.

HENSHILWOOD, C.S., F. D'ERRICO, R. YATES, Z. JACOBS, C. TRIBOLO, G.A.T. DULLER, N. MERCIER, J.C. SEALY, H. VALLADAS, I. WATTS & A.G. WINTLE. 2002. Emergence of modern human behavior: Middle Stone Age engravings from South Africa. *Science* 295: 1278–1280.

HENSHILWOOD, C.S., K.L. VAN NIEKERK, S. WURZ, A. DELAGNES, S.J. ARMITAGE, R.F. RIFKIN, K. DOUZE, P. KEENE, M.M. HAALAND, J. REYNARD, E. DISCAMPS & S.S. MIENIES. 2014. Klipdrift Shelter, southern Cape, South Africa: preliminary report on the Howiesons Poort layers. *Journal of Archaeological Science* 45: 284–303.

HODGSKISS, T. 2014. Cognitive requirements for ochre use in the Middle Stone Age at Sibudu, South Africa. *Cambridge Archaeological Journal* 24: 405–428.

HOVERS, E., B. VANDERMEERSCH & O. BAR-YOSEF. 1997. A Middle Paleolithic engraved artefact from Qafzeh Cave, Israel. *Rock Art Research* 14: 79–87.

JAUBERT, J., F. BIGLARI, V. MOURRE, L. BRUXELLES, J.-G. BORDES, S. SHIDRANG, R. NADERI, M. MASHKOUR, B. MAUREILLE, J.-B. MALLYE & Y. QUINIF. 2009. The Middle Palaeolithic occupation of Mar-Tarik, a new Zagros Mousterian site in Bisotun massif (Kermanshah, Iran), in M. Otte, F. Biglari, & J. Jaubert (ed.) *Iran Palaeolithic Le paléolithique d'Iran*: 7–27. BAR International Series 1968. Oxford: Archaeopress.

JOORDENS, J.C.A., F. D'ERRICO, F.P. WESSELINGH, S. MUNRO, J. DE VOS, J. WALLINGA, C. ANKJÆRGAARD, T. REIMANN, J.R. WIJBRANS, K.F. KUIPER, H.J. MÜCHER, H. COQUEUGNIOT, V. PRIÉ, I. JOOSTEN, B. VAN OS, A.S. SCHULP, M. PANUEL, V. VAN DER HAAS, W. LUSTENHOUWER, J.J.G. REIJMER & W. ROEBROEKS. 2015. *Homo erectus* at Trinil on Java used shells for tool production and engraving. *Nature* 518: 228–231.

LANGLEY, M.C., C. CLARKSON & S. ULM. 2008. Behavioural complexity in Eurasian Neanderthal populations: a chronological examination of the archaeological evidence. *Cambridge Archaeological Journal* 18: 289–307.

LEONARDI, P. 1976. Les incisions pré-leptolithiques du Riparo Tagliente (Verone) et de Terra Amata (Nice) en relation au problème de la naissance de l'art. *Atti della Accademia Nazionale dei Lincei* 8: 35–104.

— 1981. Raschiatoio musteriano del Riparo Solinas di Fumane (Verona) con incisioni sul cortice. *Atti dell'Accademia Roveretana degli Agiati Contributi della Classe di Scienze Umane, Lettere e Arti* 20: 87–92.

— 1983. Incisioni e segni vari paleolitici del Riparo Tagliente di Stallavena nei Monti Lessini presso Verona (Italia). Campagne di scavo 1972-1982. *Atti del Museo Civico di Storia Naturale di Trieste* 34: 143–176.

— 1988. Art paléolithique mobilier et pariétal en Italie. *L'Anthropologie* 92: 139–202.

L'HOMME, V. & E. NORMAND. 1993. Présentation des galets striés de la couche inférieure du gisement moustérien de 'Chez Pourré-Chez Comte' (Corrèze). *Paléo* 5: 121–25.

LI, H., Z. LI, M.G. LOTTER & K. KUMAN. Formation processes at the early Late Pleistocene archaic human site of Lingjing, China. *Journal of Archaeological Science*, in press.

LI, Z. 2007. A primary study on the stone artifacts of Lingjing site excavated in 2005. *Acta Anthropologica Sinica* 26: 138–154.

LI, Z. & W. DONG. 2007. Mammalian fauna from the Lingjing Paleolithic site in Xuchang, Henan Province. *Acta Anthropologica Sinica* 26: 345–360.

LI, Z., D. KUNIKITA & S. KATO. 2017. Early pottery from the Lingjing site and the emergence of pottery in northern China. *Quaternary International* 441: 49–61.

LI, Z. & H. MA. 2016. Techno-typological analysis of the microlithic assemblage at the Xuchang Man site, Lingjing, central China. *Quaternary International* 400: 120–129.

LI, Z., X. WU, L. ZHOU, W. LIU, X. GAO, X. NIAN & E. TRINKAUS. 2017. Late Pleistocene archaic human crania from Xuchang, China. *Science* 355: 969–972.

MACKAY, A. & A. WELZ. 2008. Engraved ochre from a Middle Stone Age context at Klein Kliphuis in the Western Cape of South Africa. *Journal of Archaeological Science* 35: 1521–1532.

MAJKIĆ, A., F. D'ERRICO, S. MILOŠEVIĆ, D. MIHAILOVIĆ & V. DIMITRIJEVIĆ. 2018a. Sequential incisions on a cave bear bone from the Middle Paleolithic of Pešturina Cave, Serbia. *Journal of Archaeological Method and Theory* 25: 69–116.

MAJKIĆ, A., F. D'ERRICO & V. STEPANCHUK. 2018b. Assessing the significance of Palaeolithic engraved cortexes: a case study from the Mousterian site of Kiik-Koba, Crimea. *PLOS ONE* 13: e0195049.

MANIA, D. & U. MANIA. 1988. Deliberate engravings on bone artefacts of *Homo erectus*. *Rock Art Research* 5: 91–95.

MARSHACK, A. 1976. Some implications of the Paleolithic symbolic evidence for the origin of language. *Current Anthropology* 17: 274–282.

— 1990. Early hominid symbol and evolution of the human capacity, in P.A. Mellars (ed.) *The emergence of modern humans: and archaeological perspective*: 457–98. Ithaca: Cornell University Press.

MAUREILLE, B., A. MANN, C. BEAUVAL, J.G. BORDES, L. BOURGUIGNON, S. COSTAMAGNO, I. COUCHOUD, M.D. GARRALDA, E.-M. GEIGL, J. FAUQUIGNON, F. LACRAMPE-CUYAUBÈRE, R. GRÜN, P. GUIBERT, V. LAROULANDIE, J.-C. MARQUET, L. MEIGNEN, C. MUSSINI, W. RENDU, A. ROYER, G. SEGUIN & J.-P. TEXIER. 2010. Les Pradelles à Marillac-le-Franc (Charente). Fouilles 2011-2007: nouveaux résultats et synthèse, in J. Buisson-Catil & J. Primault (ed.) *Préhistoire entre Vienne et Charente. Hommes et sociétés du Paléolithique. Association des publications chauvinoises, Mém. XXXVIII*: 145–162. Chauvigny: APC.

NIAN, X.M., L.P. ZHOU & J.T. QIN. 2009. Comparisons of equivalent dose values obtained with different protocols using a lacustrine sediment sample from Xuchang, China. *Radiation Measurements* 44: 512–516.

PENG, F., X. GAO, H. WANG, F. CHEN, D. LIU & S. PEI. 2012. An engraved artifact from Shuidonggou, an early Late Paleolithic site in Northwest China. *Chinese Science Bulletin* 57: 4594–4599.

PERESANI, M., S. DALLATORRE, P. ASTUTI, M.C. DAL, S. ZIGGIOTTI & C. PERETTO. 2014. Symbolic or utilitarian? Juggling interpretations of Neanderthal behavior: new inferences from the study of engraved stone surfaces. *Journal of anthropological sciences* 92: 233–255.

RODRÍGUEZ-VIDAL, J., F. D'ERRICO, F.G. PACHECO, R. BLASCO, J. ROSELL, R.P. JENNINGS, A. QUEFFELEC, G. FINLAYSON, D.A. FA, J.M.G. LÓPEZ, J.S. CARRIÓN, J.J. NEGRO, S. FINLAYSON, L.M. CÁCERES, M.A. BERNAL, S.F. JIMÉNEZ & C. FINLAYSON. 2014. A rock engraving made by Neanderthals in Gibraltar. *Proceedings of the National Academy of Sciences* 111: 13301–13306.

SIRAKOV, N., J.-L. GUADELLI, S. IVANOVA, S. SIRAKOVA, M. BOUDADI-MALIGNE, I. DIMITROVA, F. PH, C. FERRIER, A. GUADELLI, D. IORDANOVA, N. IORDANOVA, M. KOVATCHEVA, I. KRUMOV, J.-C. LEBLANC, V. MITEVA, V. POPOV, R. SPASSOV, S. TANEVA & T. TSANOVA. 2010. An ancient continuous human presence in the Balkans and the beginnings of human settlement in western Eurasia: A Lower Pleistocene example of the Lower Palaeolithic levels in Kozarnika cave (North-western Bulgaria). *Quaternary International* 223–224: 94–106.

STEPANCHUK, V.N. 1993. Prolom II, a Middle Palaeolithic cave site in the Eastern Crimea with non-utilitarian bone artefacts. *Proceedings of the Prehistoric Society* 59: 17–37.

— 2006. *The Lower and Middle Paleolithic of Ukraine*. Chernovtsy: Zelena Bukovina.

TEXIER, P.-J., G. PORRAZ, J. PARKINGTON, J.-P. RIGAUD, C. POGGENPOEL, C. MILLER, C. TRIBOLO, C. CARTWRIGHT, A. COUDENNEAU, R. KLEIN, T. STEELE & C. VERNA. 2010. A Howiesons Poort tradition of engraving ostrich eggshell containers dated to 60,000 years ago at Diepkloof Rock Shelter, South Africa. *Proceedings of the National Academy of Sciences* 107: 6180–6185.

VINCENT, A. 1988. L'os comme artefact au Paléolithique moyen: principes d'étude et premiers résultats, in M. Otte, L. Binford & J.P. Rigaud (ed.) *L'homme de Néandertal 4, La technique*: 185–196. Liège: ERAUL.

VOGELSANG, R., J. RICHTER, Z. JACOBS, B. EICHHORN, V. LINSEELE & R.G. ROBERTS. 2010. New excavations of Middle Stone Age deposits at Apollo 11 rockshelter, Namibia: stratigraphy, archaeology, chronology and past environments. *Journal of African Archaeology* 8: 185–218.

WANG, W., Z. LI, G. SONG & Y. WU. 2015. A study of possible Hyaena coprolites from the Lingjing Site, Central China. *Acta Anthropologica Sinica* 34: 117–125.

WANG, W., Y. WU, G. SONG, K. ZHAO & Z. LI. 2014. Pollen and fungi spore analysis on Hyaenid coprolite from the Xuchang Man Site, Central China. *Chinese Science Bulletin* 58: 51–56.

WATTS, I. 2010. The pigments from Pinnacle Point Cave 13B, Western Cape, South Africa. *Journal of Human Evolution* 59: 392–411.

ZHANG, S., X. GAO, Y. ZHANG & Z. LI. 2011. Taphonomic analysis of the Lingjing fauna and the first report of a Middle Paleolithic kill-butchery site in North China. *Chinese Science Bulletin* 56: 3213–3219.

ZHANG, S., Z. LI, Y. ZHANG & X. GAO. 2012. Skeletal element distributions of the large herbivores from the Lingjing site, Henan Province, China. *Science China: Earth Sciences* 55: 246–253.

ZILHÃO, J. 2007. The emergence of ornaments and art: an archaeological perspective on the origins of "behavioral modernity". *Journal of Archaeological Research* 15: 1–54.